

# Vanishing opinions in Latané model of opinion formation

Maciej Dworak and Krzysztof Malarz\*

AGH University of Science and Technology, Faculty of Physics and Applied Computer Science,  
al. Mickiewicza 30, 30-059 Kraków, Poland

(Dated: December 13, 2022)

In this paper, the results of computer simulations based on Nowak–Szamrej–Latané model with multiple (from two to five) opinions available in the system are presented. We introduce the noise discrimination level (which says how small the clusters of agents could be considered as negligible) as a quite useful quantity that allows qualitative characterization of the system. We show that depending on the introduced noise discrimination level, the range of actors’ interactions (controlled indirectly by an exponent in distance scaling function, the larger the exponent the more influential the nearest neighbors are) and the information noise level (modeled as social temperature, which increases results in increase of randomness in taking the opinion by the agents), the ultimate number of the opinions (measured as the number of clusters of actors sharing the same opinion in clusters greater than the noise discrimination level) may be smaller than the number of opinions available in the system. These are observed in small and large information noise limits but result in either unanimity, or polarization, or randomization of opinions.

Keywords: sociophysics; social impact; opinion dynamics; clusterization and polarization; information noise

## I. INTRODUCTION

The formation and dynamics of opinions [1–11] and its spread and propagation [12, 13] seem to be a vivid section of sociophysics [14–20]. Existing models [21, 22] may be grouped into two families: with discrete or continuous opinions. The latter are represented by Hegselmann–Krause model [23–25], Deffuant *et al.* model [26–30] (in a one-dimensional opinion space), the Zaller–Deffuant model [31–34] (in a two-dimensional opinion space), compromise model [35–37] or others [38, 39]. In the family of discrete models, a particular role is played by toy models dealing with binary opinions and simplified rules of opinion formation, with majority [40, 41], voter [42–44], Sznajd [45–49], Galam [50, 51] models, among others.

For example, in the voter model [42], the opinions of any given actor on some issue change at random times under the influence of the opinions of his/her neighbors. An actor’s opinion at any given time can take one of two values. At random times, a random individual is selected, and that actor’s opinion is changed according to a stochastic rule. Specifically, for one of the chosen actor’s neighbors, one is chosen according to a given set of probabilities, and that individual’s opinion is transferred to the chosen actor.

In the majority model [40], at each time step, a group of  $r$  actors is selected, where  $r$  can be constant or changed in each successive step. All randomly selected actors adopt the opinion that dominates the group. If the size  $r$  of a group of neighbors is even, in case of a tie, either the group adopts an arbitrarily determined biased opinion or maintains the *status quo*.

In the original one-dimensional version of the Sznajd model [45] agent in position  $i$  adopts the opinion of the

actor sitting in position  $i + 2$  and the actor in position  $i + 1$  adopts the opinion of the actor sitting in position  $i - 1$ . These rules ultimately lead system to one of three (stable and fixed) attracting points: either two states of *unanimity* or one state of alternately opposite opinions (‘antiferromagnetic’ state).

These models may be particularly useful for modeling the thinking dichotomy, that is, binary thinking that involves only two extreme attitudes<sup>1</sup>. Such a situation occurs for voters in countries with two-parties systems (like in USA), or for actors answering fundamental or simple questions. For example, people usually well know if they like chicken livers with onion (or not), people usually well know if they believe that our Earth is flat (or not), people usually well know if they are pro or contra abortion, etc.

Somewhere on the border between two (discrete/continuous) families of models, discrete opinion models allow multiple opinions to appear [52–63]. These models still allow us to observe geometrical *clusterization* of opinions, but also their *polarization*, which is naturally forced (assumed) in the case of models with binary opinions. Such models are particularly attractive for modeling indifferents as an interface between pro and contra, modeling responses to Likert-scale questionnaires<sup>2</sup>, or modeling voter decisions in multiparty systems.

Here, we use a discrete multi-choice opinion model based on computerized version [64] of opinion formation based on Latané theory of social impact [65–67] (see References 55, 56, 68–70 for examples of model applications

<sup>1</sup> Typical answers (measuring opinions) for dichotomy-like questionnaires are: ‘No’ and ‘Yes’.

<sup>2</sup> Typical answers (measuring opinions) for Likert-like questionnaires are: ‘Strongly disagree’, ‘Disagree’, ‘Neither agree nor disagree’, ‘Agree’ and ‘Strongly agree’.

\*  0000-0001-9980-0363; malarz@agh.edu.pl

and Reference 71 for a comprehensive review).

In Reference 55 Nowak–Szamrej–Latané model [64] was modified to allow multiple (more than two) opinions. It was shown that in the presence of information noise (modeled as social temperature  $T$ ) the signatures of order/disorder phase transition were observed: in the average fraction of actors sharing the  $i$ -th opinion; its variation; average number of clusters of actors with the same opinion and the average size of the largest cluster of actors who share the same opinion. The social temperature  $T$  played a role as a standard Boltzmann distribution parameter that contains the social impact as the equivalent of energy. The order and disordered phases were observed for low ( $T < T_C$ ) and high ( $T > T_C$ ), respectively. For a homogeneous society (with identical actors' supportiveness and persuasiveness) the critical social temperature  $T_C$  decreased with increasing number of available opinions  $K$ .

The authors of Reference 56 showed that opinion formation and spread were influenced by both: *i*) flow of information between actors (effective range of interactions between actors) and *ii*) randomness in adopting opinions (noise level). Noise not only leads to opinions disorder, but also promotes consensus under certain conditions. In the disordered phase and when the exchange of information is spatially effectively limited, various faces of disorder were observed, including system states, where the signatures of self-organized criticality manifested themselves as a scale-free probability distribution function for sizes of cluster of actors sharing the same opinion. Then increasing the noise level leads the system to a disordered random state. The critical noise level  $T_C$  above which the histograms of the sizes of the opinion groups lost their scale-free character increases with an increase in the ease of information flow.

In this paper, we continue the studies presented in References 55 and 56. Namely, with computer simulation based on Nowak–Szamrej–Latané model [64] we check: *i*) how influential are the nearest neighbors with respect to the entire population; *ii*) the opinion clusterization (including the distribution of these cluster numbers and their sizes); *iii*) and distribution of surviving opinions.

The rest of the paper is organized as follows. In Section II a detailed description of the model is presented. Section III contains the results of simulations. The results obtained are discussed in Section IV and summarized in Section V. The list of references and three appendixes—presenting detailed results on: examples of final spatial opinion distribution (Appendix A); average number of clusters (Appendix B); the number of surviving opinions (Appendix C)—close the manuscript.

## II. MODEL

The model is based on previous attempts [55, 56, 70, 72, 73] to describe the dynamics of opinion in the context of the theory of social impact [65–67] in its computerized

version [64]. The system contains  $N$  actors labeled with  $i = 0, \dots, N - 1$ . Every actor  $i$  at time  $t$  has an opinion  $\xi_i(t) \in \Xi$ . The set  $\Xi$  of available opinions consists of  $K$  different opinions  $\{\Xi_1, \dots, \Xi_K\}$ . The social impact  $\mathcal{I}_{i,k}(t)$  exerted in time  $t$  on an actor  $i$  by all actors who share opinions  $\Xi_k$  is calculated as

$$\mathcal{I}_{i,k}(t) = \sum_{j=0}^{N-1} \frac{4s_j}{g(d_{i,j})} \cdot \delta(\Xi_k, \xi_j(t)) \cdot \delta(\xi_j(t), \xi_i(t)) \quad (1a)$$

or

$$\mathcal{I}_{i,k}(t) = \sum_{j=0}^{N-1} \frac{4p_j}{g(d_{i,j})} \cdot \delta(\Xi_k, \xi_j(t)) \cdot [1 - \delta(\xi_j(t), \xi_i(t))], \quad (1b)$$

where Kronecker delta  $\delta(x, y) = 0$  when  $x \neq y$  and  $\delta(x, y) = 1$  when  $x = y$ . The term  $\delta(\Xi_k, \xi_j(t))$  in Equation (1) indicates that the impact  $\mathcal{I}_{i,k}(t)$  on the  $i$ -th agent in time  $t$  is exerted only by agents  $j$  who at time  $t$  believe in the opinion  $\Xi_k$  ( $\xi_j(t) = \Xi_k$ ). The term  $\delta(\xi_j(t), \xi_i(t))$  in Equation (1a) vanishes when  $\xi_i(t) \neq \xi_j(t)$ , i.e., it produces a non-zero contribution of the impact  $\mathcal{I}_{i,k}(t)$  on agent  $i$  only when agent  $j$  shares the opinion of agent  $i$ . Thus, term  $s_j$  is considered to be the *supportiveness* of the  $j$ -th actor. On the contrary, the term  $[1 - \delta(\xi_j(t), \xi_i(t))]$  resets the impact when agents  $i$  and  $j$  share the same opinion. It means that the components of the sum (1b) can be non-zero only when interacting in time  $t$  agents have different opinions  $\xi_i(t) \neq \xi_j(t)$  and thus  $p_j$  play a role of *persuasiveness* of the  $j$ -th agent. The supportiveness  $s_i$  and persuasiveness  $p_i$  are taken randomly from the interval  $[0, 1]$ .  $d_{i,j}$  stands for the Euclidean distance between agents  $i$  and  $j$ . The distance scaling function  $g(\cdot)$  should be a non-decreasing function that ensures a decreasing influence from more and more distant actors. Here, we assume that

$$g(x) = 1 + x^\alpha, \quad (2)$$

where the exponent  $\alpha$  is a model control parameter.

After calculating impacts (1) for each actor  $i$  and every opinion  $\Xi_k$  available in the system, the temporal evolution of  $i$ -th actor opinion  $\xi_i$  can be predicted based on either deterministic (in absence of information noise) or non-deterministic (in presence of information noise) way.

In the deterministic version (without information noise), the actor  $i$  in the next time step ( $t + 1$ ) takes the opinion  $\Xi_k$  that the believers exerted the largest impact on him/her:

$$\xi_i(t + 1) = \Xi_k \iff \mathcal{I}_{i,k}(t) = \max(\mathcal{I}_{i,1}(t), \mathcal{I}_{i,2}(t), \dots, \mathcal{I}_{i,K}(t)). \quad (3)$$

When information noise is present in the system, the social impact  $\mathcal{I}_{i,k}(t)$  (1) determines the probability  $P_{i,k}(t)$  of accepting opinion  $\Xi_k$  in the next time step ( $t + 1$ ) by  $i$ -th actor. To that end, we introduce a

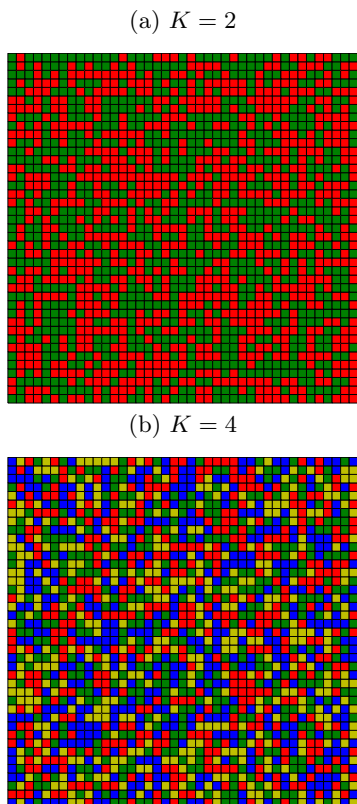


FIG. 1: Example of random initial state of the system for (a)  $K = 2$  and (b)  $K = 4$ . Various colors correspond to various opinions.

(temperature-like) information noise parameter  $T$  [74] and a Boltzmann-like factor

$$p_{i,k}(t) = \exp\left(\frac{\mathcal{I}_{i,k}(t)}{T}\right), \quad (4a)$$

which allow us to define the above-mentioned probability

$$P_{i,k}(t) = \frac{p_{i,k}(t)}{\sum_{j=1}^K p_{i,j}(t)}. \quad (4b)$$

Then,  $i$ -th actor accepts in the next time step ( $t + 1$ ) opinion  $\Xi_k$

$$\xi_i(t + 1) = \Xi_k, \text{ with probability } P_{i,k}(t). \quad (5)$$

We assume that the actors occupy nodes of the square grid

$$\mathcal{G} = \{(x, y) : 0 \leq x, y < L, \quad x, y \in \mathbb{Z}\}$$

and agent's label  $i = Lx + y$ . The open boundary conditions are assumed. Initially (at  $t = 0$ ), the agents take a random opinions. The examples of the initial system states are presented in Figure 1 for  $K = 2$  (Figure 1a) and for  $K = 4$  (Figure 1b). Various opinions are marked by various colors. The algorithm of performed simulations is presented in Algorithm 1 [73]. The source code of program (written in C) is available in Reference 75.

### III. RESULTS

In this Section we describe the results of computer simulations carried for square lattice with  $L^2 = 41^2$  actors. If not stated otherwise the results are gathered after  $t = 1000$  time steps and averaged over  $R = 100$  independent system realizations (for various random initial spatial distribution of opinions  $\xi_i(t = 0)$ , supportiveness  $s_i$  and persuasiveness  $p_i$  values).

#### A. How influential are the nearest-neighbours in respect to the entire population?

To better understand the role played by the  $\alpha$  parameter, we check the ratio

$$\beta(n) = \frac{(L - 2r)^{-2} \cdot \sum_{x=r}^{(L-r)} \sum_{y=r}^{(L-r)} \sum_{k=1}^K \mathcal{I}_{i,k}^n(t \rightarrow \infty)}{L^{-2} \cdot \sum_{i=1}^{L^2} \sum_{k=1}^K \mathcal{I}_{i,k}(t \rightarrow \infty)}, \quad (6)$$

which describes the opinion-independent relative influence of  $n$  geometrically nearest neighbors with respect to the total impact coming from all actors. Examples of shapes of these nearest neighborhoods containing  $n = 1, 9, 25, 49$  actors are sketched in Figure 2. The measured influence ratio  $\beta(n)$  is averaged over  $(L - 2r)^2$  actors with  $r = 0$  for  $n = 1$ ,  $r = 1$  for  $n = 9$ ,  $r = 2$  for  $n = 25$ ,  $r = 3$  for  $n = 49$ , etc., reflecting the possibility of placing the yellow square from Figure 2 in the square grid  $\mathcal{G}$  without protruding beyond the boundaries of the system. The term  $\mathcal{I}_{i,k}^n$  stands for social impact calculated according to Equation (1) but with an upper summation index replaced by  $(n - 1)$  instead of  $(N - 1)$ . The impacts  $\mathcal{I}_{i,k}^n$  and  $\mathcal{I}_{i,k}$  are measured at the long-term simulation limit ( $t \rightarrow \infty$ ). The results of the simulations of  $\beta(n)$  are presented in Table I.

Within the estimated uncertainties, the ratio  $\beta(n)$  does not depend on the number  $K$  of opinions available in the system and appears to be a purely geometric characteristic of the model. Of course, we expected an observed increase of  $\beta(n)$  with an increase of  $n$  independently on  $K$  and  $\alpha$ . Much more interesting is the observed monotonic increase of  $\beta(n)$  with the increase of the distance scaling function exponent  $\alpha$ . For  $\alpha = 2$  roughly 25% of the impact comes from  $n = 9$  nearest-neighbors. This ratio increases to  $\beta(9) \approx 59\%$  for  $\alpha = 3$ ,  $\beta(9) \approx 80\%$  for  $\alpha = 4$  and  $\beta(9) \approx 96\%$  for  $\alpha = 6$ . For  $n = 25$  roughly  $\beta(25) \approx 39\%$ ,  $76\%$ ,  $92\%$  and  $99\%$  of the social impact exerted comes from only those twenty five neighbors for  $\alpha = 2, 3, 4$  and  $6$ , respectively. In other words, the  $\alpha$  parameter says how influential the nearest neighbors are with respect to the entire population: the larger  $\alpha$  the more influential the nearest neighbors are.

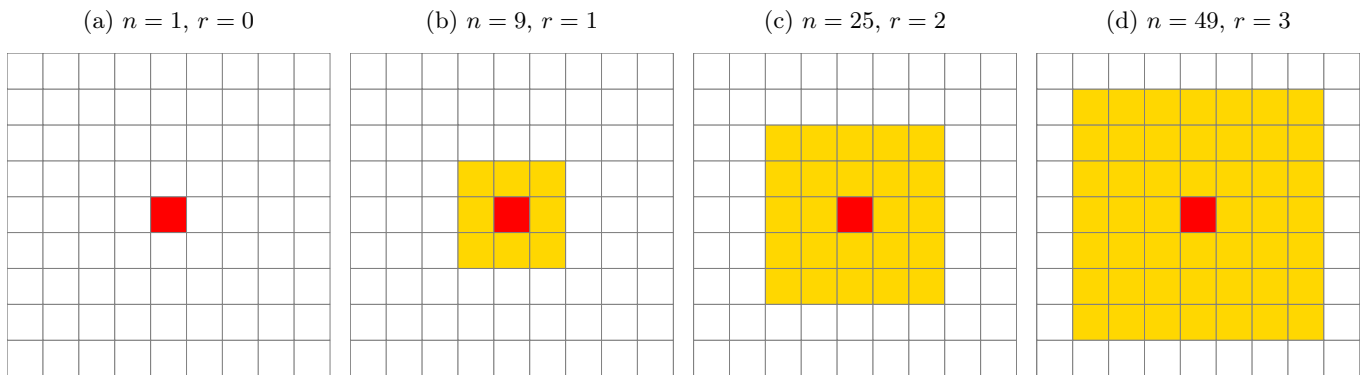


FIG. 2: The sketches of shapes of the neighborhoods closest to the sites (a)  $n = 1$ , (b)  $n = 9$ , (c)  $n = 25$ , (d)  $n = 49$  sites. The values of the  $r$  parameters indicated in the figures in the headline influence summation limits in the nominator of Equation (6).

### B. The final opinions distributions

The initial random opinions presented in Figure 1 evolve according to Equation (3) (in the absence of information noise  $T = 0$ ) or Equation (5) (for  $T > 0$ ). This temporal evolution subsequently changes the spatial opinion distribution. In Figure 3 examples of two most probable final opinion spatial distributions for various noise levels  $T$  after  $10^3$  time steps are presented. The exponent in the distance scaling function is assumed to be  $\alpha = 3$ . The system contains  $L^2 = 41^2$  actors and  $K = 4$  possible opinions.

For a deterministic version of algorithm ( $T = 0$ , see Figures 3a and 3b) all  $K$  opinions initially present in the systems survive, however, the clustering of actors who share the same opinions is observed. Slight increase of temperature ( $T = 1$ ) ‘melts’ the ‘frozen’ state leading either to consensus (the same opinion shared by all actors, see Figure 3c) or polarization (two, well separated, clusters of opinions, see Figure 3d). As a cluster of opinions—or more precisely actors—we consider a group of actors who share the same opinions and connected by the nearest-neighbor interaction (sitting in the von Neumann neighborhood, as for random site percolation problem). The number of actors who share the same opinion and belong to the same cluster defines the cluster size  $\mathcal{S}$ . The increase of noise level to  $T = 2$  allows a small number of actors to appear with other available but short-lived opinions (appearing at time  $t$  and immediately disappearing at  $t+1$ ) (see Figures 3e and 3f) as the temperature increases  $T$ —according to Equation (4)—favorites the appearance of less probable opinions (exerting less impact). The above-mentioned increase of probability (4) with  $T$  leads to an increase of the number of single actors or even pairs of actors with minority opinions destroying locally either consensus (see Figure 3g) or system polarization (see Figure 3h). The further increase in  $T$  also allows for the appearance of larger (but still relatively small) clusters of opinions (Figures 3i and 3j). Finally, for a high

noise level, all opinions become equiprobable as

$$\lim_{T \rightarrow \infty} P_{i,k}(t) = 1/K$$

in every time step  $t$  for every actor  $i$  and for every opinion  $\Xi_k$ . The latter leads to the system blinking with all  $K$  available ‘colors of opinion at every time step  $t$  and at every site  $i$ —the snapshot of the system does not differ much from the one presented in Figure 1b.

Examples of the spatial distributions of the final opinion for  $\alpha = 3$  and  $K = 2, 3$  and  $5$  (Figures 8 to 10) and for  $\alpha = 4$  and  $K = 2, 3, 4$  and  $5$  (Figures 11 to 14) are collected in Appendix A.

### C. Opinion clustering

As the most common observed phenomenon in the system is opinion clustering, we check the distribution of these cluster numbers and sizes. To this end, we utilize the Hoshen–Kopelman algorithm [76, pp. 59–60], [77–79]. With Hoshen–Kopelman algorithm, one can label every site in such a way that sites (actors sharing the same opinions) in various clusters are labeled with various labels and sites belonging to a given cluster are labeled with the same label.

Let us look again at Figures 3c and 3d obtained for  $\alpha = 3$ ,  $K = 4$  and  $T = 1$ . In Figure 3c consensus takes place and we observe a single cluster (the number of clusters  $\mathcal{C} = 1$ ) and all actors belong to this cluster (the size of the cluster  $\mathcal{S} = L^2$ ). In Figure 3d the system polarization is observed, thus the number of observed clusters is two ( $\mathcal{C} = 2$ ), but most of the actors are in a ‘red’ cluster ( $\mathcal{S}_1 \approx 0.92L^2$ ) while actors with minority opinion (marked with ‘green’) are occupying upper left corner of the system ( $\mathcal{S}_2 \approx 0.08L^2$ ).

As for larger noise level single sites with minority opinions appear from time to time (cf. for example Figures 3e to 3h) but the main picture behind remains the same (i.e. in principle we still deal either with consensus or system polarization), it would be useful to introduce the

TABLE I: Average ratio  $\beta(n)$  [defined in Equation (6)] of the influence of the neighborhood with  $n$  sites (presented in Figure 2) to the total influence of the entire network with  $L^2$  sites for various values of  $K$  and  $\alpha$ .

| $\alpha$ | 2           | 3           | 4            | 6              |
|----------|-------------|-------------|--------------|----------------|
| $n$      | $K = 2$     |             |              |                |
| 1        | 0.05987(13) | 0.14973(63) | 0.2209(13)   | 0.2902(16)     |
| 9        | 0.25269(45) | 0.58795(79) | 0.80513(74)  | 0.95820(21)    |
| 25       | 0.39642(56) | 0.76437(75) | 0.92761(38)  | 0.993687(41)   |
| 49       | 0.49898(57) | 0.84573(64) | 0.96450(21)  | 0.998328(12)   |
| 81       | 0.57600(53) | 0.89073(54) | 0.97971(13)  | 0.9994007(45)  |
| 121      | 0.63641(46) | 0.91866(44) | 0.987262(83) | 0.9997408(20)  |
| 169      | 0.68530(41) | 0.93739(36) | 0.991477(58) | 0.9998727(10)  |
| 225      | 0.72578(35) | 0.95064(29) | 0.994033(42) | 0.99993158(54) |
| 289      | 0.75989(31) | 0.96039(24) | 0.995680(31) | 0.99996061(31) |
| 361      | 0.78903(28) | 0.96778(20) | 0.996790(23) | 0.99997609(18) |
| $n$      | $K = 3$     |             |              |                |
| 1        | 0.05990(17) | 0.15080(92) | 0.2232(16)   | 0.2937(22)     |
| 9        | 0.25275(62) | 0.5873(15)  | 0.8041(10)   | 0.95793(26)    |
| 25       | 0.39649(85) | 0.7635(13)  | 0.92698(53)  | 0.993625(52)   |
| 49       | 0.49906(96) | 0.8449(11)  | 0.96414(29)  | 0.998311(15)   |
| 81       | 0.5761(10)  | 0.89006(90) | 0.97950(18)  | 0.9993947(53)  |
| 121      | 0.6365(10)  | 0.91812(72) | 0.98712(12)  | 0.9997382(22)  |
| 169      | 0.6854(10)  | 0.93694(59) | 0.991385(81) | 0.9998715(10)  |
| 225      | 0.72586(96) | 0.95027(48) | 0.993969(57) | 0.99993091(62) |
| 289      | 0.75996(93) | 0.96008(39) | 0.995633(41) | 0.99996022(35) |
| 361      | 0.78909(88) | 0.96753(32) | 0.996755(31) | 0.99997585(21) |
| $n$      | $K = 4$     |             |              |                |
| 1        | 0.05990(16) | 0.15095(98) | 0.2247(20)   | 0.2962(27)     |
| 9        | 0.25275(50) | 0.5871(15)  | 0.80338(98)  | 0.95757(28)    |
| 25       | 0.39649(65) | 0.7633(14)  | 0.92657(51)  | 0.993549(51)   |
| 49       | 0.49906(70) | 0.8448(11)  | 0.96393(29)  | 0.998291(15)   |
| 81       | 0.57609(70) | 0.88999(90) | 0.97938(18)  | 0.9993876(54)  |
| 121      | 0.63649(69) | 0.91807(74) | 0.98705(12)  | 0.9997353(22)  |
| 169      | 0.68538(66) | 0.93690(60) | 0.991331(79) | 0.9998701(12)  |
| 225      | 0.72586(63) | 0.95024(49) | 0.993931(56) | 0.99993012(63) |
| 289      | 0.75997(59) | 0.96006(41) | 0.995605(40) | 0.99995976(36) |
| 361      | 0.78911(56) | 0.96751(34) | 0.996735(30) | 0.99997557(21) |
| $n$      | $K = 5$     |             |              |                |
| 1        | 0.05988(15) | 0.1511(10)  | 0.2248(21)   | 0.2976(26)     |
| 9        | 0.25267(48) | 0.5867(15)  | 0.8029(11)   | 0.95741(29)    |
| 25       | 0.39638(58) | 0.7629(13)  | 0.92634(61)  | 0.993525(55)   |
| 49       | 0.49893(59) | 0.8445(11)  | 0.96380(34)  | 0.998284(15)   |
| 81       | 0.57595(57) | 0.88970(90) | 0.97930(21)  | 0.9993847(57)  |
| 121      | 0.63634(55) | 0.91784(73) | 0.98700(14)  | 0.9997340(25)  |
| 169      | 0.68523(53) | 0.93673(60) | 0.991302(92) | 0.9998694(12)  |
| 225      | 0.72571(51) | 0.95010(49) | 0.993909(65) | 0.99992979(66) |
| 289      | 0.75982(49) | 0.95995(40) | 0.995590(46) | 0.99995958(37) |
| 361      | 0.78896(49) | 0.96742(33) | 0.996723(35) | 0.99997546(24) |

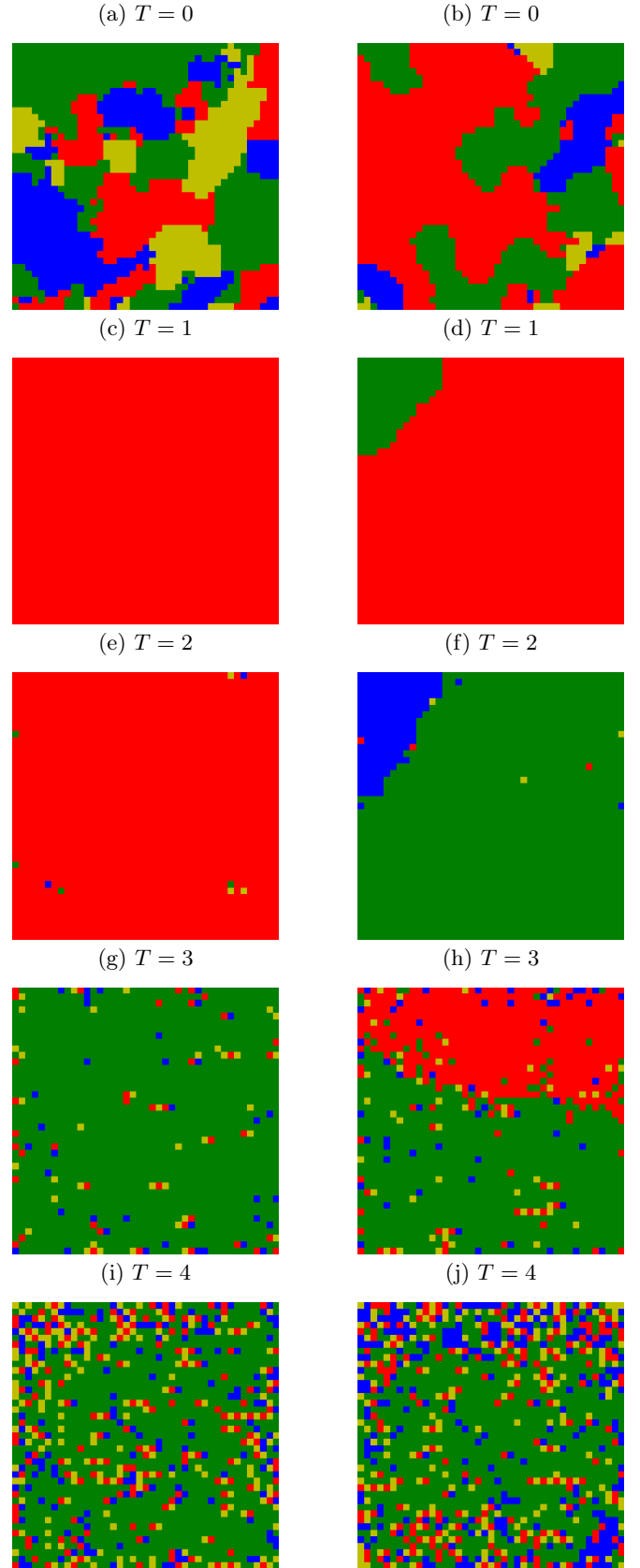


FIG. 3: Examples of two most probable spatial distributions of the final opinion after  $10^3$  time steps.  $L = 41$ ,  $\alpha = 3$ ,  $K = 4$  and various levels of noise  $T$ .

noise discrimination level  $\theta$ . For example, setting  $\theta = 5$  and neglecting appearance clusters with sizes  $\mathcal{S}$  smaller than  $\theta$  is sufficient to keep the picture of the number  $\mathcal{C}$  of clusters as for those presented in Figures 3c and 3d also for systems presented in Figures 3e to 3h.

The results presented below are based on assuming various levels of discrimination  $\theta$  in the spirit described above. In other words, the  $\theta$  parameter arbitrarily says how small the clusters of agents sharing the same opinion could be considered as negligible.

### 1. Average number of opinion clusters

In Figure 4 the average number  $\mathcal{C}$  of opinion groups is presented for  $\alpha = 3$  and  $K = 4$ . Statistics are based on  $R = 100$  replications of the system with  $L^2 = 41^2$  actors measured after  $t = 10^3$  time steps of evolution. We assume the discrimination threshold  $\theta = 25$ .

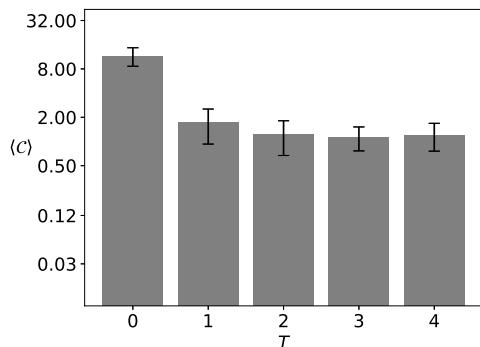


FIG. 4: Average number  $\langle \mathcal{C} \rangle$  of opinion clusters after  $t = 10^3$  time steps for the exponent of the distance scaling function  $\alpha = 3$ , the number  $K = 4$  of opinions available in the system, and the noise discrimination threshold  $\theta = 25$ . The system contains  $L^2 = 41^2$  actors. The results are averaged over  $R = 100$  independent system realizations.

For  $T = 1$  roughly half among  $R = 100$  simulations end in consensus ( $\mathcal{C} = 1$ ) or system polarization ( $\mathcal{C} = 2$ ) leading to the average number of clusters  $\langle \mathcal{C} \rangle \approx 1.73(80)$ . The symbol  $\langle \dots \rangle$  stands for the averaging procedure on  $R = 100$  independent system realizations (simulations). The increase in the level of noise  $T \geq 2$  with the assumed discrimination threshold  $\theta = 25$  does not change the average number of clusters  $\langle \mathcal{C} \rangle$  to much:  $\langle \mathcal{C} \rangle = 1.24(57)$ ,  $1.14(38)$  and  $1.22(46)$  for  $T = 2, 3$  and  $4$ , respectively.

However, for  $T = 0$  this number  $\langle \mathcal{C} \rangle \approx 11.6$  (with uncertainty 3.0) is much higher than for  $T \neq 0$  (please note the logarithmic scale on the  $\langle \mathcal{C} \rangle$  axis). We should stress that the number of clusters  $\mathcal{C} = 17$  (Figure 3a) and  $\mathcal{C} = 8$  (Figure 3b) is higher than the number of opinions available  $K = 4$  in the systems. In other words, several different clusters of the same opinion are counted for the number  $\mathcal{C}$ . For instance, in Figure 3b we observe four

clusters (of sizes  $\mathcal{C}$  larger than  $\theta = 25$ ) of ‘green’ opinions, two of ‘blue’ opinions, two of ‘red’ opinions, and none of ‘yellow’ opinions.

The average number  $\langle \mathcal{C} \rangle$  of clusters for various values of the distance scaling function exponent  $\alpha = 2, 3, 4$  and  $6$ , number of available opinions  $K = 2, 3, 4$  and  $5$ , information noise level  $T = 0, 1, 2, 3$  and  $4$  and noise discrimination levels  $\theta = 12, 25$  and  $50$  are presented in Figures 15 to 17 in Appendix B.

### 2. The sizes of the largest clusters

In Reference 56 average largest cluster size  $\langle \mathcal{S}_{\max} \rangle$  (normalized to the system size  $L^2$ ) for  $K = 2$  and  $K = 3$  and various values of the noise level  $T$  and the interaction range  $\alpha$  were presented in Figures 6a and 7a, respectively. Here, we also extend this study to a larger number  $K$  of opinions available in the system, namely for  $K = 4$  and  $K = 5$ . The results are presented in Figure 5.

Let us again look at the thermal evolution of  $\mathcal{S}_{\max}$  of the system presented in Figure 3. Due to the freezing system for  $T = 0$  (as presented in Figures 3a and 3b) the largest cluster sizes are around  $\mathcal{S}_{\max} = 267$  and  $\mathcal{S}_{\max} = 794$  (cluster of ‘green’ opinion in the upper left corner and cluster of ‘red’ opinion in the left side of Figures 3a and 3b, respectively). The increase in noise level to  $T = 1$  increases the sizes of the largest cluster to  $\mathcal{S}_{\max} = L^2$  and  $\mathcal{S}_{\max} = 1540$  for Figures 3c and 3d, respectively. Then, the subsequent increase in  $T$  only reduces the size of the largest cluster.

## D. Distribution of surviving opinions

The methodology of clusters counting allowing for construction of histograms  $\langle \mathcal{C}(T) \rangle$  presented in Figures 4 and 15 to 17—as mentioned in Section III C 1—neglects the clusters colors. Thus, the information provided there is insufficient to determine whether all  $K$  opinions available in the system persisted until the assumed time  $t = 10^3$ . Now, we are interested in checking the number  $1 \leq \Phi \leq K$  of surviving opinions for various values of the parameters  $K, \alpha$ , and  $T$ .

As mentioned above, the system presented in Figure 3b for  $K = 4, \alpha = 3, T = 0$  has eight clusters larger than  $\theta = 25$ , and thus the number of clusters  $\mathcal{C}$  is eight. As three opinions available in the system are observed, then  $\Phi = 3$ . In contrast, for  $T = 1$  (see Figure 3d) only  $\Phi = 2$  opinions (‘red’ and ‘green’) survived. There, due to the polarization of the system, the number of clusters  $\mathcal{C}$  and the number of surviving opinions  $\Phi$  are equal.

### 1. Histograms of surviving opinions

The opinion that survives in the system is the opinion that, at the end of the simulation, it is represented by at

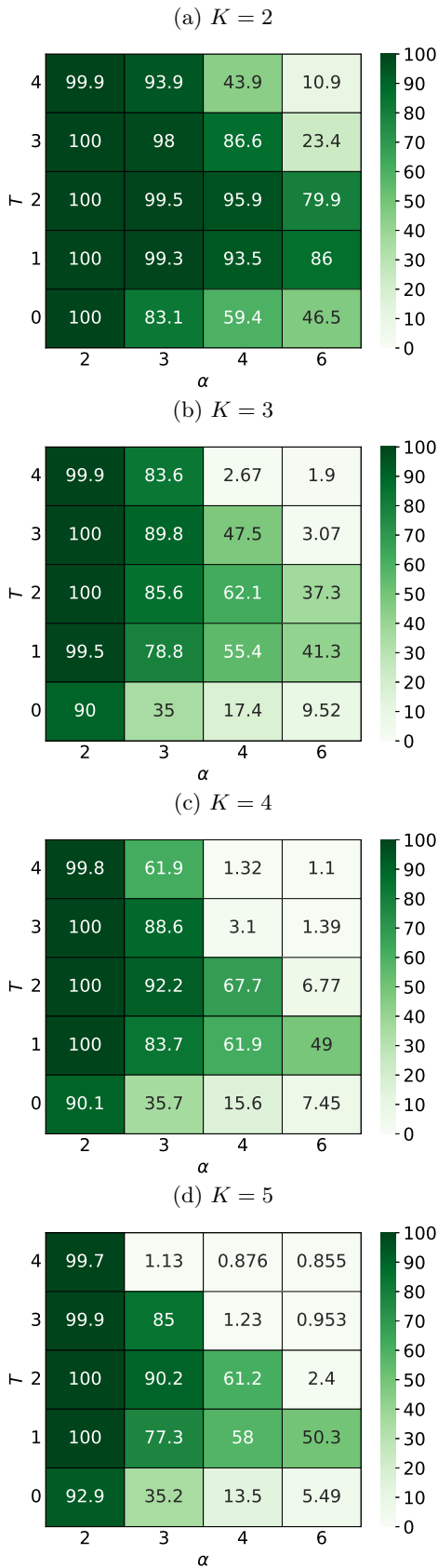


FIG. 5: The average ratio (in percents) of the size of the largest cluster  $\langle \mathcal{S}_{\max} \rangle$  to the size of the entire system  $L^2$  depending on the parameters  $\alpha$  and  $T$ .  $L = 41$ ,  $t = 10^3$ ,  $R = 100$ .

least one cluster with a size  $\mathcal{S}$  not smaller than  $\theta$ .

In Figure 6 the histogram of the number  $\Phi(T)$  of surviving opinions for  $\alpha = 3$ ,  $K = 4$  and the level of noise discrimination  $\theta = 25$  are presented.

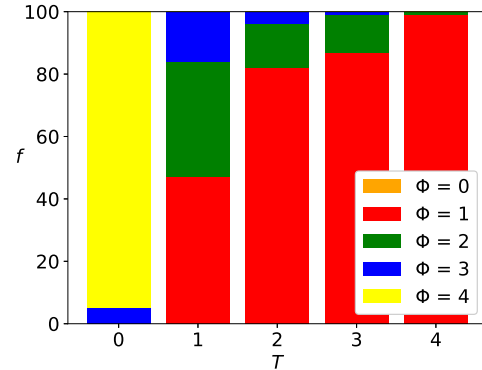


FIG. 6: The histogram of frequencies  $f$  of the number  $\Phi$  of surviving opinions for  $\alpha = 3$ ,  $K = 4$  and the level of noise discrimination  $\theta = 25$ .

The results are collected again after  $t = 10^3$  time steps and for  $R = 100$  system realizations.

For  $T = 0$ , 95% of these  $R$  simulations ended with  $\Phi = 4$  [ $f(\Phi = 4) = 95\%$ , yellow rectangle in the first bar of Figure 6] surviving opinions, and 5% of the simulations ended with  $\Phi = 3$  surviving opinions [ $f(\Phi = 3) = 5\%$ , blue rectangle in the first bar of Figure 6]. Situations with consensus ( $\Phi = 1$ ) or system polarization ( $\Phi = 2$ ) were not observed:  $f(\Phi = 1) = f(\Phi = 2) = 0\%$  [absence of green and red rectangles in the first bar of Figure 6]. Finally, the orange color is also absent [ $f(\Phi = 0) = 0\%$ ] in the first bar of Figure 6] which means that the situation of all opinions disappearing was not observed. Of course, the rules of the game do not allow for vanishing all opinions: the case  $f(\Phi = 0) > 0$  means that the fraction  $f(\Phi = 0)$  of system realizations ended with a lot of very small clusters, each of them smaller than the assumed noise discrimination level  $\theta$ .

For  $T = 1$ , 47% of these  $R$  simulations ended with  $\Phi = 1$  [ $f(\Phi = 1) = 47\%$ , red rectangle on the second bar of Figure 6] surviving opinions, 37% of the simulations ended with  $\Phi = 2$  surviving opinions [ $f(\Phi = 2) = 37\%$ , green rectangle in the second bar of Figure 6] and 16% of the simulations ended with  $\Phi = 3$  surviving opinions [ $f(\Phi = 3) = 16\%$ , blue rectangle in the second bar of Figure 6], etc.

For the highest noise level investigated ( $T = 4$ ) we have  $f(\Phi = 1) \approx 99\%$  (red rectangle in the fifth bar in Figure 6) and  $f(\Phi = 2) \approx 1\%$  (green rectangle in the fifth bar in Figure 6).

Histograms of frequencies  $f(\Phi)$  of the numbers  $\Phi$  of the surviving opinions for various values of  $K$ ,  $\alpha$ ,  $T$  and three values of noise discrimination level  $\theta = 12, 25, 50$  are presented in Figures 18 to 20 in Appendix C.

## 2. The most probable number of surviving opinions

We finalize the presentation of the results with heat maps of the most probable final number of surviving opinions  $\Phi^*$  (see Figure 7). We define the most probable number of surviving opinions  $\Phi^*$  as this value of  $\Phi$  for which the fraction  $f(\Phi)$  is the largest (for fixed values of the noise discrimination level  $\theta$ , the noise level of information  $T$  and the effective range of interaction  $\alpha$ ).

For example, for  $K = 4$ ,  $\alpha = 3$ ,  $\theta = 25$  and

- for  $T = 0$  (see the first bar of Figure 6)  $\Phi^* = 4$  as  $95\% = f(\Phi = 4) > f(\Phi = 3) = 5\%$ ,
- for  $T = 1, 2, 3$  (see the second, third, and fourth bar of Figure 6)  $\Phi^* = 1$  as  $f(\Phi = 1) > f(\Phi = 2) > f(\Phi = 3)$ ,
- for  $T = 4$  (see the fifth bar of Figure 6)  $\Phi^* = 1$  as  $99\% = f(\Phi = 1) > f(\Phi = 2) = 1\%$ .

## IV. DISCUSSION

### A. Average number of opinion clusters

For a low value of the noise discrimination level ( $\theta = 12$ , Figure 15) and  $\alpha = 2$  (see Figures 15a to 15d) for the nondeterministic version of the algorithm ( $T > 0$ ), only one cluster exceeds the threshold size, regardless of the number  $K$  of opinions available in the system. Therefore, the system is dominated by a single group of opinions, and consensus takes place.

Reducing the impact of distant actors ( $\alpha = 3$ , Figures 15e to 15h) allows additional clusters of size  $S$  greater than  $\theta = 12$ . Their number  $\langle \mathcal{C} \rangle$  most often does not exceed two, except for the simulation of a high number of opinions available ( $K > 3$ ) and high social temperature ( $T = 4$ ). For such parameter settings, we can observe on average more than two clusters, at the same time with a greater standard deviation of this number — the number of clusters, depending on the simulation, ranges from  $\langle \mathcal{C} \rangle = 1$  to about  $\langle \mathcal{C} \rangle = 5 \div 6$ . Independently of the number of  $K$  the deterministic case ( $T = 0$ ) produces a relatively high average number  $\langle \mathcal{C} \rangle$  of clusters ( $\langle \mathcal{C} \rangle = 4$  for  $K = 2$  opinions,  $\langle \mathcal{C} \rangle = 16$  and for  $K > 2$ ).

An increased exponent ( $\alpha = 4$ , Figures 15i to 15l) results in a clear increase in the average number  $\langle \mathcal{C} \rangle$  of clusters in the system up to  $\langle \mathcal{C} \rangle = 32$  for  $T = 0$ .

For the largest value considered of  $\alpha = 6$  (Figures 15m to 15p) the most numerous sets of clusters with a size  $S$  exceeding  $\theta = 12$  are observed. With two opinions in the system (Figure 15m), the temperature  $T = 3$  is sufficient for a significant division of agents for  $\langle \mathcal{C} \rangle \geq 16$  clusters with a size exceeding the threshold  $\theta$ . The trend continues for simulations with available  $K = 3$  different opinions (Figure 15n). However, for high temperatures and a large number of possible opinions ( $K = 4$ ,  $T = 4$

and  $K = 5$ ,  $T = 3, 4$ ), the average number of clusters  $\langle \mathcal{C} \rangle$  with a size  $S$  greater than the threshold  $\theta$  begins to decline due to too much fragmentation — the system becomes an irregular set of many very small clusters (Figures 13i, 13j, 14i and 14j), and none of the opinions can get a noticeable advantage. For  $T = 0$ , the average number of clusters in the system remains very high and reaches  $\langle \mathcal{C} \rangle = 32$ .

For increased threshold  $\theta = 25$  (Figure 16) noticeable differences appear for  $K = 4, 5$  and  $\alpha = 3$  and the highest of the social temperatures studied  $T = 4$  (Figures 16g and 16h), where fewer clusters were recorded that met the condition  $S > \theta = 25$ .

For the simulations with  $K = 5$  and  $T = 4$ , where at least one cluster of an appropriate size has been preserved, it was so rare that the average number of clusters was a fraction ( $\langle \mathcal{C} \rangle \approx 0.15$ ). This value well reflects the division of agents who share the same opinion into small, randomly arranged clusters.

A further increase in the threshold  $\theta$  (up to 50, Figure 17) results in disappearing clusters of sizes  $S$  larger than  $\theta$  for  $\alpha \geq 4$  and  $K \geq 4$  (Figures 17k, 17l, 17o and 17p).

### B. The sizes of the largest clusters

We would like to recall the ambivalent role observed of the information noise level  $T$  in shaping the largest cluster size  $\mathcal{S}_{\max}$  mentioned in Reference 56, p. 14: “[...] the average size of the maximum cluster  $\mathcal{S}_{\max}$  decreases with  $\alpha$  for fixed  $T$  values. The appearance of noise in the system ( $T = 1$ ) slightly organizes the system in relation to the noiseless situation with  $T = 0$  (which is particularly visible for  $\alpha > 2$  [...]). Indeed, as in earlier studies [80, 81], small level of noise brought more order to the system. Furthermore, the introduction of noise ( $T$ ) in the adoption of opinions causes an increase in  $\mathcal{S}_{\max}$ , and then its decrease, which is especially visible for  $\alpha > 2$  (this inflection point is nearly  $T = 2$ .” and later: “[...] noise for certain values of  $\alpha$  promotes unanimity. This situation occurs for  $\alpha = 3$  (both for  $K = 2$  and  $K = 3$ ), when the frozen state system, with increasing noise  $T$ , achieves the consensus state for  $T = 3$ , before disordering for  $T = 5$ ” [56, p. 18].

This nonmonotonous dependence  $\mathcal{S}_{\max}/L^2$  on the noise parameter  $T$  is observed for any value of  $\alpha$  but for larger values of  $\alpha$  and larger values of the number  $K$  of opinions available in the systems, this dependence becomes more and more spectacular. For example, for  $K = 5$  (Figure 5d) we see a high peak of  $\mathcal{S}_{\max}/L^2 \approx 50\%$  for  $T = 1$  and  $\alpha = 6$  deeply reduced to 2.4% and 5.5% for a larger ( $T = 2$ ) and lower ( $T = 0$ ) noise level. The similar behavior in  $\mathcal{S}_{\max}$  in dependence on  $T$  is also observed for  $\alpha = 4$  with  $\mathcal{S}_{\max}/L^2 \approx 60\%$  for  $T = 1, 2$  reduced to 1.2% and 13.3% for a higher ( $T = 3$ ) and lower ( $T = 0$ ) noise level. The further increasing influence of more distance actors (decreasing  $\alpha$ ) makes the  $\mathcal{S}_{\max}$  dependence more



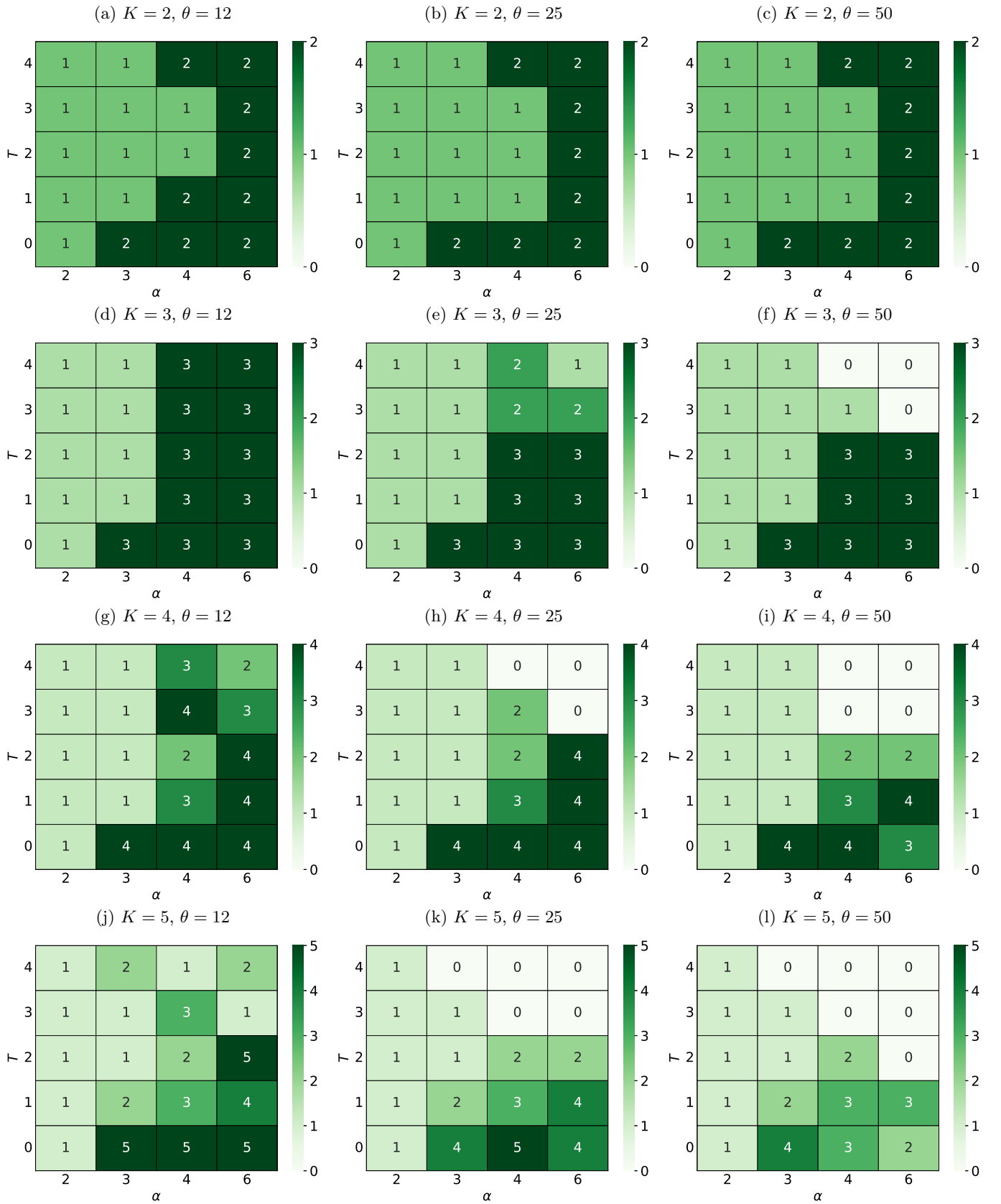


FIG. 7: The most probable final number  $\Phi^*$  of surviving opinions for various numbers  $K$  of opinions available in the system and noise discrimination thresholds  $\theta$  depending on the level of information noise  $T$  and the range of interaction  $\alpha$ .

and more smoother, making it almost flat for  $\alpha = 2$  with only marginal deviation from  $\mathcal{S}_{\max}/L^2 = 100\%$  at the edges of the range of values studied for the parameter  $T$ .

The picture presented above is also qualitatively reproduced for  $K = 4$  (see Figure 5c).

Independently of the number  $K$  of opinions considered available in the system for fixed value of the noise parameter  $T$  the average size of the largest cluster  $\mathcal{S}_{\max}$  decreases with increasing of  $\alpha$ , i.e., with limiting the influence of very long-range interactions.

### C. Histograms of surviving opinions

The histograms  $f(\Phi; T)$  of the surviving opinions (Section III D 1) presented in Figures 18 to 20 in Appendix C are almost untouched by the noise discrimination level  $\theta$  for a high effective interaction range [ $\alpha = 2$ , Figures 18a to 18d, 19a to 19d and 20a to 20d] as well as for the lowest possible number of opinions available in the system [ $K = 2$ , Figures 18a, 18e, 18i, 18m, 19a, 19e, 19i, 19m, 20a, 20e, 20i and 20m]. This is a consequence of the appearance of consensus or system polarization and is consistent with the generally observed final system states presented earlier in Figures 3 and 8 to 14.

The most noticeable differences occur in Figures 18g, 18h, 18k, 18l, 18o, 18p, 19g, 19h, 19k, 19l, 19o, 19p, 20g, 20h, 20k, 20l, 20o and 20p, that is, for  $\alpha \geq 3$  and  $K \geq 4$ . For a high noise level ( $T = 4$ ) in this parameter regime, the frequency  $f(\Phi = 0)$  dominates the system (absence of sizes  $S$  greater than  $\theta$ ) except for the lowest assumed threshold  $\theta = 12$ , allowing observation up to  $\Phi = 3$  surviving opinions, but of small cluster sizes.

### D. The most probable number of surviving opinions

We finalize the discussion of the results obtained with an analysis of the heat maps (Figure 7) of the most probable final number  $\Phi^*$  (Section III D 2, Figure 7) of the remaining opinions for various numbers  $K$  of opinions available in the system and various noise discrimination numbers  $\theta$ . These maps are constructed in the  $(\alpha, T)$  plane. With the assumed scanning accuracy of the parameters  $\alpha$  i  $T$  parameters, the shape of the obtained maps differs qualitatively from those reported in Figures 6 and 7 in Reference [56], particularly with well-visible juts for higher values of  $\Phi^*$  for intermediate values of the level of information noise  $2 \leq T \leq 3$  and high values of  $\alpha \approx 6$  (that is, for a long effective range of interaction between actors).

## V. CONCLUSION

In Reference 55 the model of opinion formation was introduced based on the Latané theory of social im-

pact with many available opinions. In computer simulations based on the Szamrej–Nowak–Latané model, it was shown that increasing the number of opinions decreases the critical noise level separating ordered and disordered phases. The observed results were followed by further studies [56] in which both the noise level  $T$  and the interaction range  $\alpha$  were considered. It was shown that the noise level has an ambiguous role: its lower value helps in system ordering (spatial clustering of opinions), while its higher value destroys any spatial correlations among actors and their opinions. This useful role for the small noise level was also reported in References 81–84.

In this paper, we follow the path indicated in the References 55 and 56 and with a computerized version of the social impact theory (Section II) we simulate the formation of opinions in an artificial society. Images obtained from spatial opinion distributions (Section III B) were analyzed in terms of the grouping of opinions and the characteristics of these opinion clusters (Section III C). Based on the simulation results, we show how the number  $\Phi^*$  of observed opinions (understood as spatial clusters of at least  $\theta$  actors sharing the same opinion) depends on the model control parameters (effective range of interaction  $\alpha$  and noise level  $T$ ). In contrast to the Reference 56—where number of (arbitrarily recognized as small or large) cluster sizes were investigated—here we introduce the noise discrimination level  $\theta$  allowing the finest analysis of histograms of cluster sizes.

As a square lattice is not best suited for modeling the social interaction, also checking another network topology seems to be a promising way for further studies. On the other hand, the square lattice naturally produces a regular ego-centered network of actors [85–87], where nodes in subsequent coordination zones may be equated with subsequent “circles” (in the ego-centered network theory terminology) containing the support clique (sites from the first and second coordination zones, Figure 2b), sympathy group (sites from the third to fifth coordination zones, the outermost “ring” in Figure 2c), affinity group (sites from the sixth to the ninth coordination zones, the outermost “ring” in Figure 2d) and active network (sites from the 10-th to 14-th coordination zones, not marked in Figure 2). Keeping the terminology of Reference 87, a “red” actor presented in Figure 2a plays the role of “ego” while actors in subsequent coordination zones are his/her “alters”. Our results (Table I) show that—independently of the number  $K$  of opinions available in the system—from 57% (low values of  $\alpha$  in Equation (2)) to 99% (high values of  $\alpha$  in Equation (2)) social impact on “ego” comes from these five circles. We note that this effect is purely geometrical and should be recognized in any other topology of the underlying network of social contacts.

The maps shown in Figures 3 and 10 indicate the tendency of the system to ultimately dominate only one opinion for  $T > 1$ . With the available opinions  $K > 3$ , by introducing a higher temperature  $T$  in the system, the share of dominant opinion in the entire system is reduced due to more spatially separated actors with dif-

ferent opinions. For the number of opinions  $K = 5$  and the social temperature  $T = 4$ , this effect is magnified to such an extent that larger clusters in the system disappear, leading to an ever-changing random system state in which none of the available opinions prevail above the noise discrimination level  $\theta$ .

High social temperature (observed, e.g. before elections) can be identified with high-mood liability, where many often consecutive events cause constant changes in individual opinions. A large part of voters do not know who to vote for, they have just started to think about it, their opinions are poorly established, and the final opinion is determined by random events.

As the exponent  $\alpha$  increases in the distance scaling function, the system tends to form more and more clusters. On the other hand, increasing the social temperature  $T$  destroys the stability of the smaller clusters that exist in the system, which disappear in favor of the dominant clusters. However, as both values increase—especially for the large number of  $K$  opinions available in the system—agents’ opinions become highly dispersed and believers of the same opinion are unable to form large clusters. For high values of  $K$ ,  $\alpha$  and  $T$  the system is fragmented, and the state of the system is represented by dynamically changing and randomly distributed clusters on the grid, and each opinion has a similar number of agents believing in it.

Increasing the discrimination coefficient decreases the importance of small—spatially separated—groups of agents sharing a given opinion in the measurement of opinions. This may contribute to the impression of strong polarization in the system, giving a vision of the presence of well-established divisions in society. This, in turn, may promote the image of a deep conflict between members of society, for example, between the voters of the two main political forces, creating the impression of a high electoral threshold. This effect is clearly visible in Figure 7, where the successive increase in  $\theta$  leads to the systematic impression that the opinions of minorities (or at least their spatial dispersion) successively decrease the measured number  $\Phi^*$  of the remaining opinions. This effect is best visible in the last row of Figure 7 (Figures 7j to 7l),

that is, for a large number of available options ( $K = 5$ ), where for the threshold  $\theta = 50$  (Figure 7l) regardless of the influence of the effective interaction range  $\alpha$  or the social temperature  $T$ , we do not observe a group of followers of the fifth opinion, and followers of the fourth opinion appear only marginally with only one of the examined sets of parameters ( $\alpha = 3$  and  $T = 0$ ). On the one hand, this can be a hint for manipulators of public opinion, and on the other hand, it can suggest how to effectively oppose such manipulation.

We emphasize that the concept of multiple opinions ( $K \geq 3$ ) seems to be essential for the possibility of speaking about system polarization (which term is probably often overused in binary models of opinion formation). Based on the results collected in Table I we conclude that the larger  $\alpha$  the more influential the nearest neighbors are (see Section III A). The level of noise discrimination  $\theta$  (allowing for detailed studies of the number  $\Phi^*$  of surviving opinions) may be a useful tool for the analysis of social systems not only in models of opinion dynamics.

The further direction of investigating this model may include checking the computational complexity, that is, the time to reach the equilibrium of the system as dependent on the size of the system or checking the influence of setting  $s_i$  and  $p_i$  in a way other than proposed here (i.e., taking them from normal instead of uniform distribution, or setting all of them to the same arbitrarily chosen values and reducing their space into only two parameters:  $\forall i : s_i = s, p_i = p$ ).

## ACKNOWLEDGMENTS

We thank Krzysztof Kułakowski for a fruitful discussion and Jacek Tarasiuk for providing a nice random number generator. We thank anonymous Reviewers for pointing out the deficiency of the original manuscript, possible directions of further research and References 35 and 39 and particularly Reference 87 as well as for encouraging us to make the source code available online [75].

- 
- [1] S. Galam, *Opinion dynamics and unifying principles: A global unifying frame*, [Entropy](#) **24**, 1201 (2022).
  - [2] I. Kozitsin, *A general framework to link theory and empirics in opinion formation models*, [Scientific Reports](#) **12**, 5543 (2022).
  - [3] T. Weron and J. Szubiński, *Opinion evolution in divided community*, [Entropy](#) **24**, 185 (2022).
  - [4] S. Galam and R. R. W. Brooks, *Radicalism: The asymmetric stances of radicals versus conventionals*, [Physical Review E](#) **105**, 044112 (2022).
  - [5] R. Muslim, M. Kholili, and A. Nugraha, *Opinion dynamics involving contrarian and independence behaviors based on the Sznajd model with two-two and three-one agent interactions*, [Physica D: Nonlinear Phenomena](#) **439**, 133379 (2022).
  - [6] Y. Lian and X. Dong, *An opinion dynamics model for unrelated discrete opinions*, [Knowledge-Based Systems](#) **251**, 109133 (2022).
  - [7] W. Su, X. Chen, Y. Yu, and G. Chen, *Noise-based control of opinion dynamics*, [IEEE Transactions on Automatic Control](#) **67**, 3134–3140 (2022).
  - [8] D. S. Zachary, *Modelling shifts in social opinion through an application of classical physics*, [Scientific Reports](#) **12**, 5485 (2022).
  - [9] V. X. Nguyen, G. Xiao, X.-J. Xu, Q. Wu, and C.-Y. Xia, *Dynamics of opinion formation under majority rules on complex social networks*, [Scientific Reports](#) **10**, 456 (2020).

- [10] S. Galam and T. Cheon, *Asymmetric contrarians in opinion dynamics*, *Entropy* **22**, 25 (2020).
- [11] S. Galam and T. Cheon, *Tipping points in opinion dynamics: A universal formula in five dimensions*, *Frontiers in Physics* **8**, 566580 (2020).
- [12] K. Malarz, Z. Szvetelszky, B. Szekfü, and K. Kułakowski, *Gossip in random networks*, *Acta Physica Polonica B* **37**, 3049–3058 (2006).
- [13] D. Choi, S. Chun, H. Oh, J. Han, and T. T. Kwon, *Rumor propagation is amplified by echo chambers in social media*, *Scientific Reports* **10**, 310 (2020).
- [14] C. Castellano, S. Fortunato, and V. Loreto, *Statistical physics of social dynamics*, *Reviews of Modern Physics* **81**, 591–646 (2009).
- [15] D. Stauffer, *A biased review of sociophysics*, *Journal of Statistical Physics* **151**, 9–20 (2013).
- [16] S. Galam, *The Trump phenomenon: An explanation from sociophysics*, *International Journal of Modern Physics B* **31**, 1742015 (2017).
- [17] A. Ishii and Y. Kawahata, *Sociophysics analysis of the dynamics of peoples' interests in society*, *Frontiers in Physics* **6**, 089 (2018).
- [18] F. Schweitzer, *Sociophysics*, *Physics Today* **71**, 40–46 (2018).
- [19] P. Sobkowicz, *Social simulation models at the ethical crossroads*, *Science and Engineering Ethics* **25**, 143–157 (2019).
- [20] M. Jusup, P. Holme, K. Kanazawa, M. Takayasu, I. Romić, Z. Wang, S. Geček, T. Lipić, B. Podobnik, L. Wang, W. Luo, T. Klanjšček, J. Fan, S. Boccaletti, and M. Perc, *Social physics*, *Physics Reports* **948**, 1–148 (2022).
- [21] S. Fortunato and D. Stauffer, *Computer simulations of opinions* (2005), arXiv:cond-mat/0501730 [cond-mat.dis-nn].
- [22] M. Grabisch and A. Rusinowska, *A survey on nonstrategic models of opinion dynamics*, *Games* **11**, 65 (2020).
- [23] R. Hegselmann and U. Krause, *Opinion dynamics and bounded confidence: Models, analysis and simulation*, *JASSS—the Journal of Artificial Societies and Social Simulation* **5**, (3)2 (2002).
- [24] H. Schawe and L. Hernández, *When open mindedness hinders consensus*, *Scientific Reports* **10**, 8273 (2020).
- [25] H. Schawe and L. Hernández, *Collective effects of the cost of opinion change*, *Scientific Reports* **10**, 13825 (2020).
- [26] G. Deffuant, D. Neau, F. Amblard, and G. Weisbuch, *Mixing beliefs among interacting agents*, *Advances in Complex Systems* **3**, 87 (2000).
- [27] G. Deffuant, *Comparing extremism propagation patterns in continuous opinion models*, *JASSS—the Journal of Artificial Societies and Social Simulation* **9**, (3)8 (2006).
- [28] K. Malarz, *Truth seekers in opinion dynamics models*, *International Journal of Modern Physics C* **17**, 1521–1524 (2006).
- [29] J.-D. Mathias, S. Huet, and G. Deffuant, *Bounded confidence model with fixed uncertainties and extremists: The opinions can keep fluctuating indefinitely*, *JASSS—the Journal of Artificial Societies and Social Simulation* **19**, (1)6 (2016).
- [30] G. Chen, H. Cheng, C. Huang, W. Han, Q. Dai, H. Li, and J. Yang, *Deffuant model on a ring with repelling mechanism and circular opinions*, *Physical Review E* **95**, 042118 (2017).
- [31] K. Kułakowski, *Opinion polarization in the Receipt–Accept–Sample model*, *Physica A* **388**, 469–476 (2009).
- [32] K. Malarz, P. Gronek, and K. Kułakowski, *Zaller–Deffuant model of mass opinion*, *JASSS—the Journal of Artificial Societies and Social Simulation* **14**, 2 (2011).
- [33] K. Malarz and K. Kułakowski, *Bounded confidence model: addressed information maintain diversity of opinions*, *Acta Physica Polonica A* **121**, B86–B88 (2012).
- [34] K. Malarz and K. Kułakowski, *Mental ability and common sense in an artificial society*, *Europhysics News* **45**, 21–23 (2014).
- [35] G. Weisbuch, G. Deffuant, F. Amblard, and J.-P. Nadal, in *Heterogenous Agents, Interactions and Economic Performance*, edited by R. Cowan and N. Jonard (Springer Berlin Heidelberg, Berlin, Heidelberg, 2003) pp. 225–242.
- [36] E. Ben-Naim, P. L. Krapivsky, and S. Redner, *Bifurcations and patterns in compromise processes*, *Physica D: Nonlinear Phenomena* **183**, 190–204 (2003).
- [37] E. Ben-Naim, P. L. Krapivsky, F. Vazquez, and S. Redner, *Unity and discord in opinion dynamics*, *Physica A: Statistical Mechanics and its Applications* **330**, 99–106 (2003).
- [38] G. Weisbuch, G. Deffuant, F. Amblard, and J.-P. Nadal, *Meet, discuss, and segregate!*, *Complexity* **7**, 55–63 (2002).
- [39] M. F. Laguna, G. Abramson, and D. H. Zanette, *Minorities in a model for opinion formation*, *Complexity* **9**, 31–36 (2004).
- [40] S. Galam, *Minority opinion spreading in random geometry*, *European Physical Journal B* **25**, 403–406 (2002).
- [41] L. S. Oliveira, A. C. Rodrigues, and F. L. Forgerini, *Reputation in majority rule model leading to democratic states*, *Journal of Physics: Conference Series* **1391**, 012042 (2019).
- [42] R. A. Holley and T. M. Liggett, *Ergodic theorems for weakly interacting infinite systems and voter model*, *Annals of Probability* **3**, 643–663 (1975).
- [43] F. W. S. Lima and K. Malarz, *Majority-vote model on  $(3, 4, 6, 4)$  and  $(3^4, 6)$  Archimedean lattices*, *International Journal of Modern Physics C* **17**, 1273–1283 (2006).
- [44] J. Fernandez-Gracia, K. Suchecki, J. J. Ramasco, M. San Miguel, and V. M. Eguiluz, *Is the voter model a model for voters?*, *Physical Review Letters* **112**, 158701 (2014).
- [45] K. Sznajd-Weron and J. Sznajd, *Opinion evolution in closed community*, *International Journal of Modern Physics C* **11**, 1157–1165 (2000).
- [46] K. Sznajd-Weron, *Sznajd model and its applications*, *Acta Physica Polonica B* **36**, 2537–2547 (2005).
- [47] K. Sznajd-Weron and J. Sznajd, *Who is left, who is right?*, *Physica A* **351**, 593–604 (2005).
- [48] K. Malarz and K. Kułakowski, *The Sznajd dynamics on a directed clustered network*, *Acta Physica Polonica A* **114**, 581–588 (2008).
- [49] K. Sznajd-Weron, J. Sznajd, and T. Weron, *A review on the Sznajd model—20 years after*, *Physica A* **565**, 125537 (2021).
- [50] S. Galam, *Unifying local dynamics in two-state spin systems* (2004), arXiv:cond-mat/0409484 [cond-mat.dis-nn].
- [51] S. Galam, *Sociophysics: A review of Galam models*, *International Journal of Modern Physics C* **19**, 409–440 (2008).
- [52] S. Gekle, L. Peliti, and S. Galam, *Opinion dynamics in a three-choice system*, *European Physical Journal B* **45**, 569–575 (2005).

- [53] K. Malarz and K. Kułakowski, *Indifferents as an interface between contra and pro*, *Acta Physica Polonica A* **117**, 695–699 (2010).
- [54] M. K. ÖZTÜRK, *Dynamics of discrete opinions without compromise*, *Advances in Complex Systems* **16**, 1350010 (2013).
- [55] P. Bańcerowski and K. Malarz, *Multi-choice opinion dynamics model based on Latané theory*, *European Physical Journal B* **92**, 219 (2019).
- [56] A. Kowalska-Styczeń and K. Malarz, *Noise induced unanimity and disorder in opinion formation*, *Plos One* **15**, e0235313 (2020).
- [57] A. C. R. Martins, *Discrete opinion dynamics with  $M$  choices*, *The European Physical Journal B* **93**, 1 (2020).
- [58] B. Zubillaga, A. Vilela, M. Wang, R. Du, G. Dong, and H. Stanley, *Three-state majority-vote model on small-world networks*, *Scientific Reports* **12**, 282 (2022).
- [59] L. Li, A. Zeng, Y. Fan, and Z. Di, *Modeling multi-opinion propagation in complex systems with heterogeneous relationships via Potts model on signed networks*, *Chaos* **32**, 083101 (2022).
- [60] M. Doniec, A. Lipiecki, and K. Sznajd-Weron, *Consensus, polarization and hysteresis in the three-state noisy  $q$ -voter model with bounded confidence*, *Entropy* **24**, 983 (2022).
- [61] F. Xiong, Y. Liu, L. Wang, and X. Wang, *Analysis and application of opinion model with multiple topic interactions*, *Chaos* **27**, 083113 (2017).
- [62] S. Galam, *The drastic outcomes from voting alliances in three-party democratic voting (1990–2013)*, *Journal of Statistical Physics* **151**, 46–68 (2013).
- [63] D. Wu and K. Y. Szeto, *Analysis of timescale to consensus in voting dynamics with more than two options*, *Physical Review E* **97**, 042320 (2018).
- [64] A. Nowak, J. Szamrej, and B. Latané, *From private attitude to public opinion: A dynamic theory of social impact*, *Psychological Review* **97**, 362–376 (1990).
- [65] J. M. Darley and B. Latané, *Bystander intervention in emergencies—Diffusion of responsibility*, *Journal of Personality and Social Psychology* **8**, 377–383 (1968).
- [66] B. Latané and S. Harkins, *Cross-modality matches suggest anticipated stage fright a multiplicative power function of audience size and status*, *Perception & Psychophysics* **20**, 482–488 (1976).
- [67] B. Latané, *The psychology of social impact*, *American Psychologist* **36**, 343–356 (1981).
- [68] K. Kacperski and J. A. Hołyst, *Phase transitions as a persistent feature of groups with leaders in models of opinion formation*, *Physica A* **287**, 631–643 (2000).
- [69] J. A. Hołyst, K. Kacperski, and F. Schweitzer, *Phase transitions in social impact models of opinion formation*, *Physica A* **285**, 199–210 (2000).
- [70] A. Kowalska-Styczeń and K. Malarz, in *Proceedings of the 36th International Business Information Management Association Conference*, edited by K. S. Soliman (International Business Information Management Association, 2020) pp. 10691–10698.
- [71] J. A. Hołyst, K. Kacperski, and F. Schweitzer, in *Annual Reviews of Computational Physics IX*, edited by D. Stauffer (World Scientific, Singapore, 2011) pp. 253–273.
- [72] P. Bańcerowski, *Modeling of opinion formation based on Latané theory*, Master’s thesis, AGH University of Science and Technology, Kraków (2017), in Polish.
- [73] M. Dworak, *Modeling of public opinion dynamics in a system with many available discrete opinions*, Master’s thesis, AGH University of Science and Technology, Kraków (2022), in Polish.
- [74] K. Kułakowski, [arXiv:0807.0711 \[physics.soc-ph\]](https://arxiv.org/abs/0807.0711) (2008).
- [75] [http://www.zis.agh.edu.pl/app/MSc/Maciej\\_Dworak/](http://www.zis.agh.edu.pl/app/MSc/Maciej_Dworak/).
- [76] D. P. Landau and K. Binder, *A Guide to Monte Carlo Simulations in Statistical Physics*, 3rd ed. (Cambridge University Press, 2009).
- [77] J. Hoshen and R. Kopelman, *Percolation and cluster distribution. 1. Cluster multiple labeling technique and critical concentration algorithm*, *Physical Review B* **14**, 3438–3445 (1976).
- [78] S. Frijters, T. Krüger, and J. Harting, *Parallelised Hoshen–Kopelman algorithm for lattice-Boltzmann simulations*, *Computer Physics Communications* **189**, 92–98 (2015).
- [79] M. Kotwica, P. Gronek, and K. Malarz, *Efficient space virtualisation for Hoshen–Kopelman algorithm*, *International Journal of Modern Physics C* **30**, 1950055 (2019).
- [80] J. Ren, W.-X. Wang, and F. Qi, *Randomness enhances cooperation: A resonance-type phenomenon in evolutionary games*, *Physical Review E* **75**, 045101 (2007).
- [81] H. Shirado and N. A. Christakis, *Locally noisy autonomous agents improve global human coordination in network experiments*, *Nature* **545**, 370–374 (2017).
- [82] L. De Sanctis and T. Galla, *Effects of noise and confidence thresholds in nominal and metric axelrod dynamics of social influence*, *Physical Review E* **79**, 046108 (2009).
- [83] A. E. Biondo, A. Pluchino, and A. Rapisarda, *The beneficial role of random strategies in social and financial systems*, *Journal of Statistical Physics* **151**, 607–622 (2013).
- [84] W. Su, G. Chen, and Y. Hong, *Noise leads to quasi-consensus of Hegselmann–Krause opinion dynamics*, *Automatica* **85**, 448–454 (2017).
- [85] R. Dunbar, C. Gamble, and J. Gowlett, *Social Brain, Distributed Mind* (British Academy, 2010).
- [86] A. Sutcliffe, R. Dunbar, J. Binder, and H. Arrow, *Relationships and the social brain: Integrating psychological and evolutionary perspectives*, *British Journal of Psychology* **103**, 149–168 (2012).
- [87] V. Arnaboldi, M. Conti, M. La Gala, A. Passarella, and F. Pezzoni, *Ego network structure in online social networks and its impact on information diffusion*, *Computer Communications* **76**, 26–41 (2016).

## Appendix A: Examples of final spatial opinion distribution

Examples of the two most probable spatial distributions of the final opinion after  $t = 10^3$  time steps of the system evolution for various noise levels  $T$ . The system contains  $L^2 = 41^2$  actors. The exponent of the distance scaling function  $\alpha = 3$  and the number of available opinions  $K = 2$  (Figure 8),  $\alpha = 3$  and  $K = 2$  (Figure 9),  $\alpha = 3$  and  $K = 5$  (Figure 10),  $\alpha = 4$  and  $K = 2$  (Figure 11),  $\alpha = 4$  and  $K = 3$  (Figure 12),  $\alpha = 4$  and  $K = 4$  (Figure 13),  $\alpha = 4$  and  $K = 5$  (Figure 14).

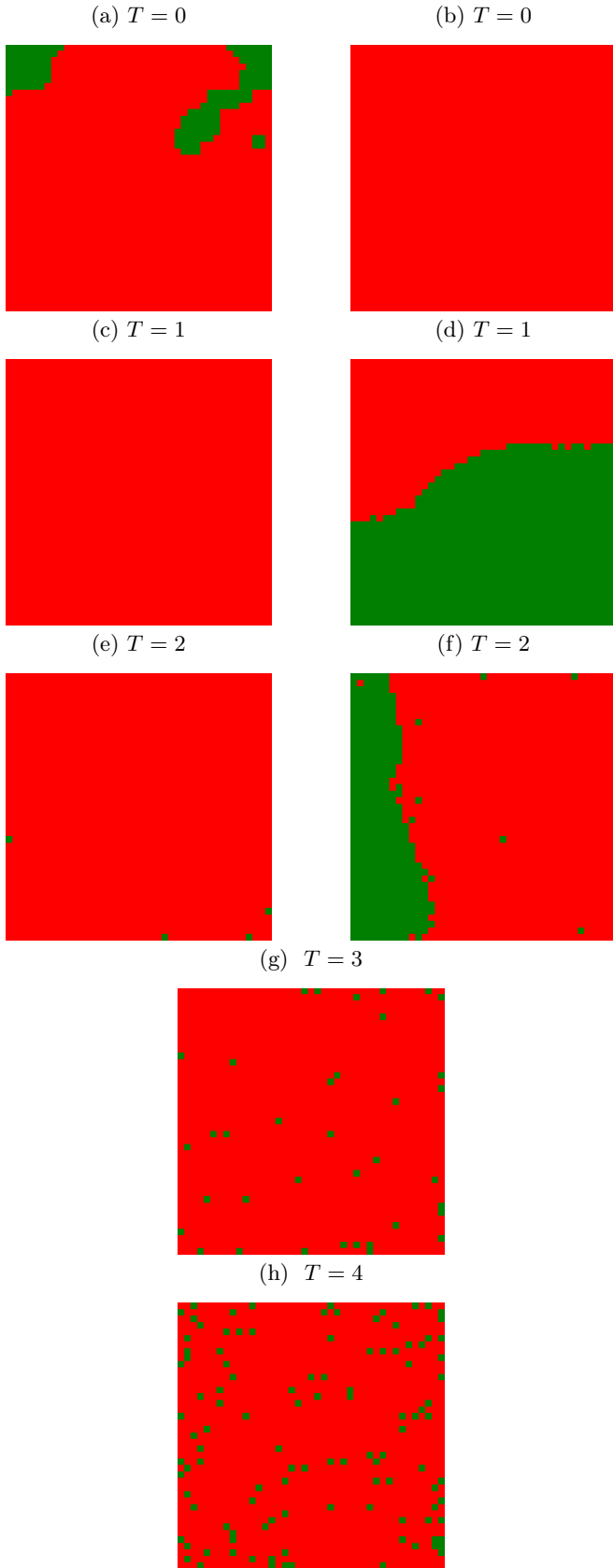


FIG. 8: Examples of two most probable spatial distributions of the final opinion after  $10^3$  time steps.  $L = 41$ ,  $\alpha = 3$ ,  $K = 2$  and various levels of noise  $T$ .

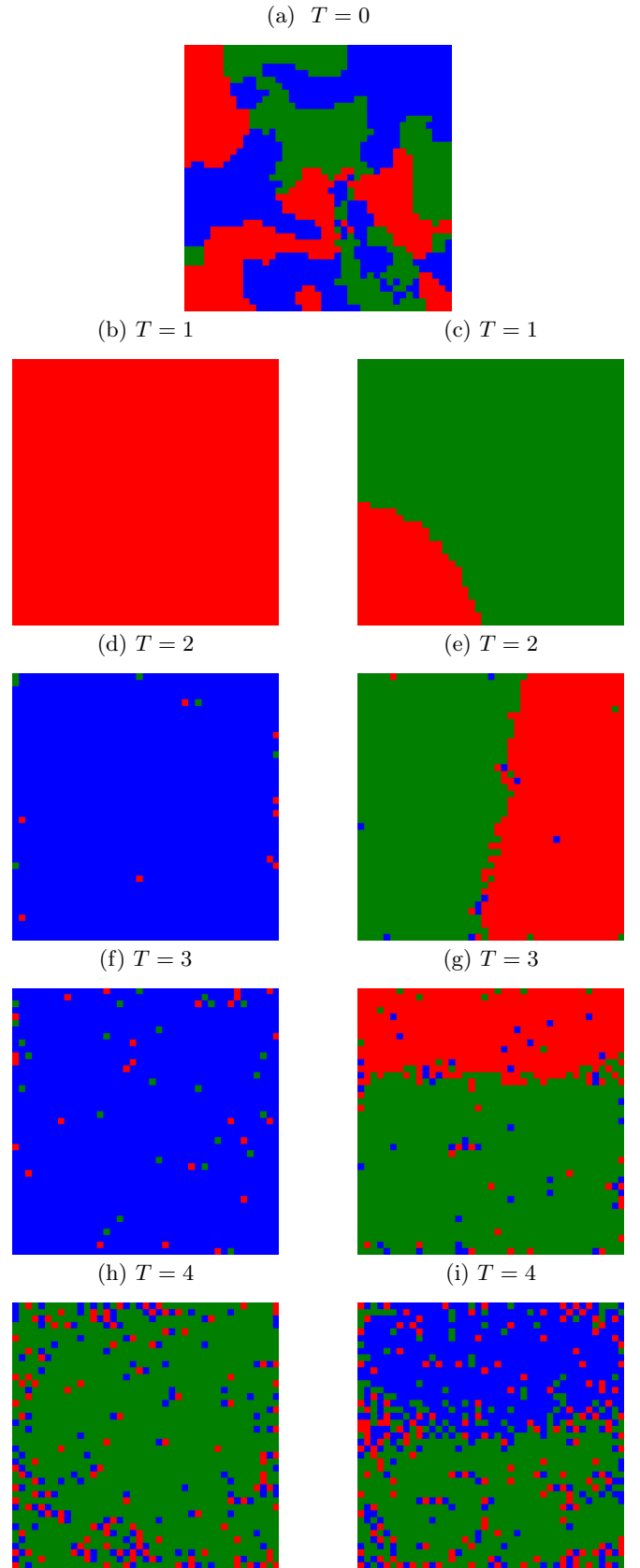


FIG. 9: Examples of two most probable spatial distributions of the final opinion after  $10^3$  time steps.  $L = 41$ ,  $\alpha = 3$ ,  $K = 3$  and various levels of noise  $T$ .

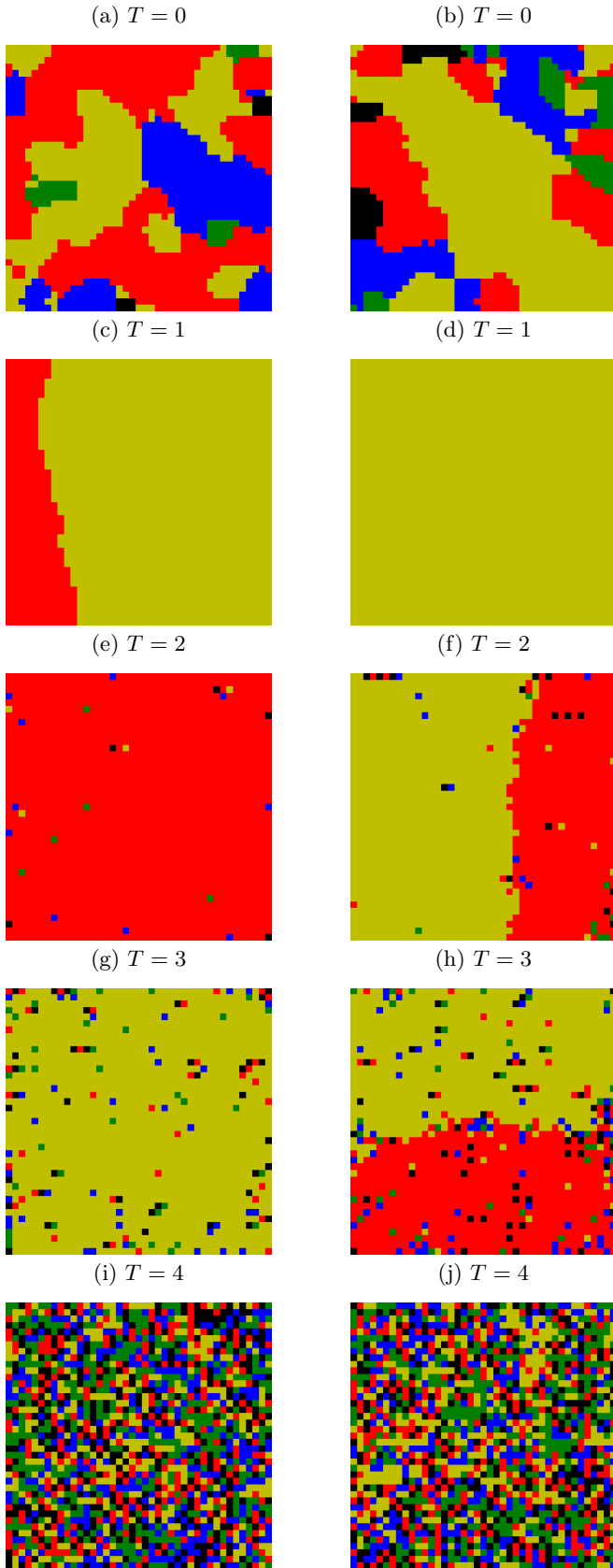


FIG. 10: Examples of two most probable spatial distributions of the final opinion after  $10^3$  time steps.  $L = 41$ ,  $\alpha = 3$ ,  $K = 5$  and various levels of noise  $T$ .

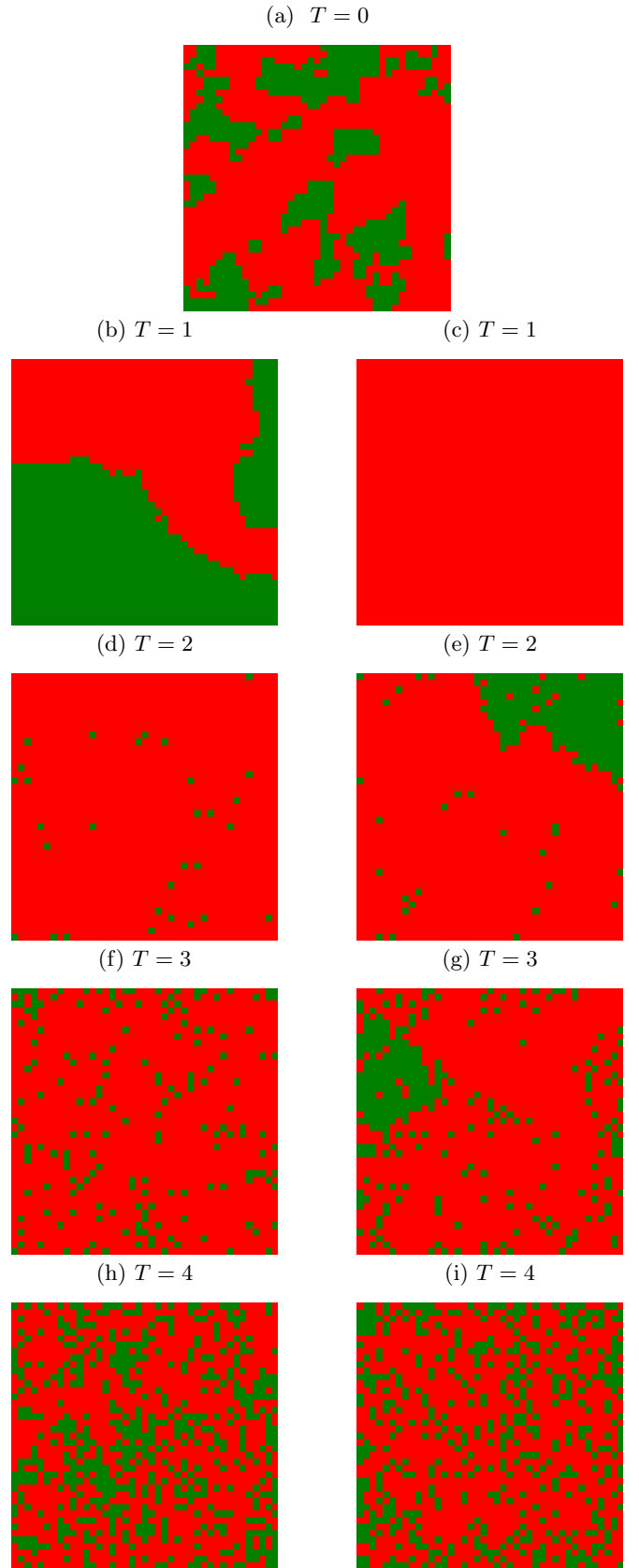


FIG. 11: Examples of two most probable spatial distributions of the final opinion after  $10^3$  time steps.  $L = 41$ ,  $\alpha = 4$ ,  $K = 2$  and various levels of noise  $T$ .

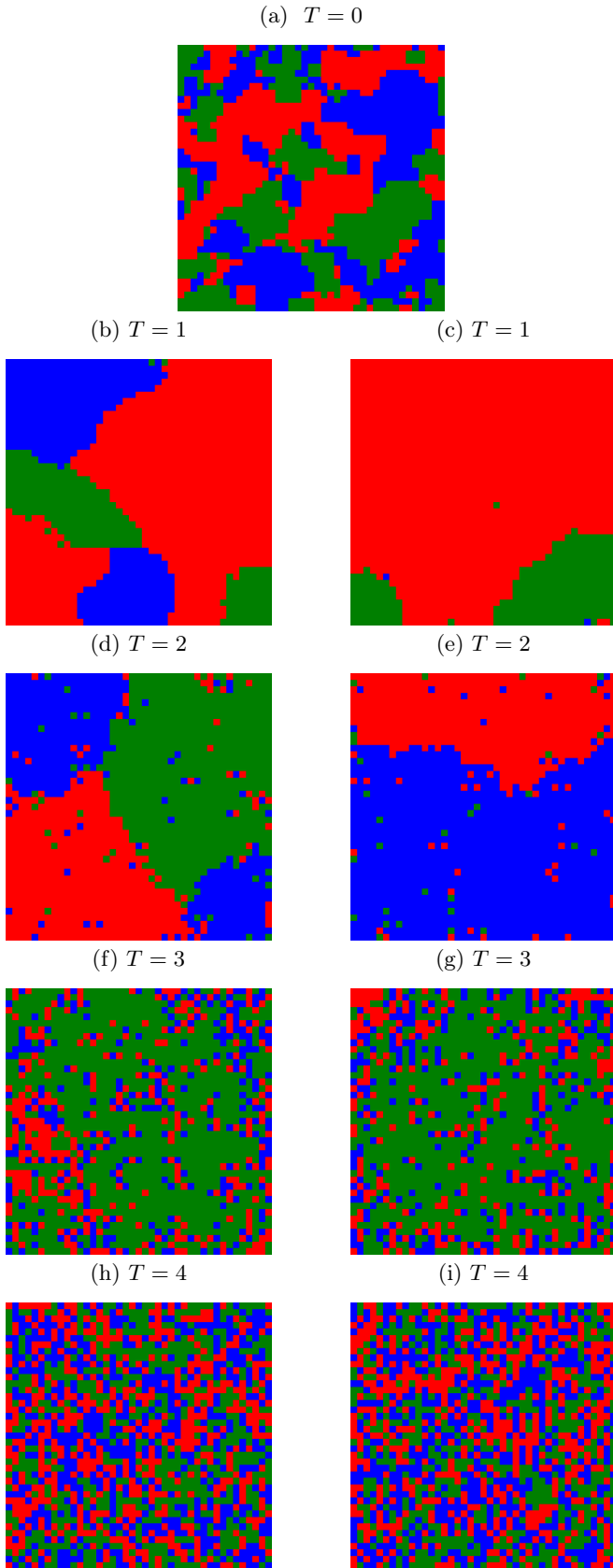


FIG. 12: Examples of two most probable spatial distributions of the final opinion after  $10^3$  time steps.  $L = 41$ ,  $\alpha = 4$ ,  $K = 3$  and various levels of noise  $T$ .

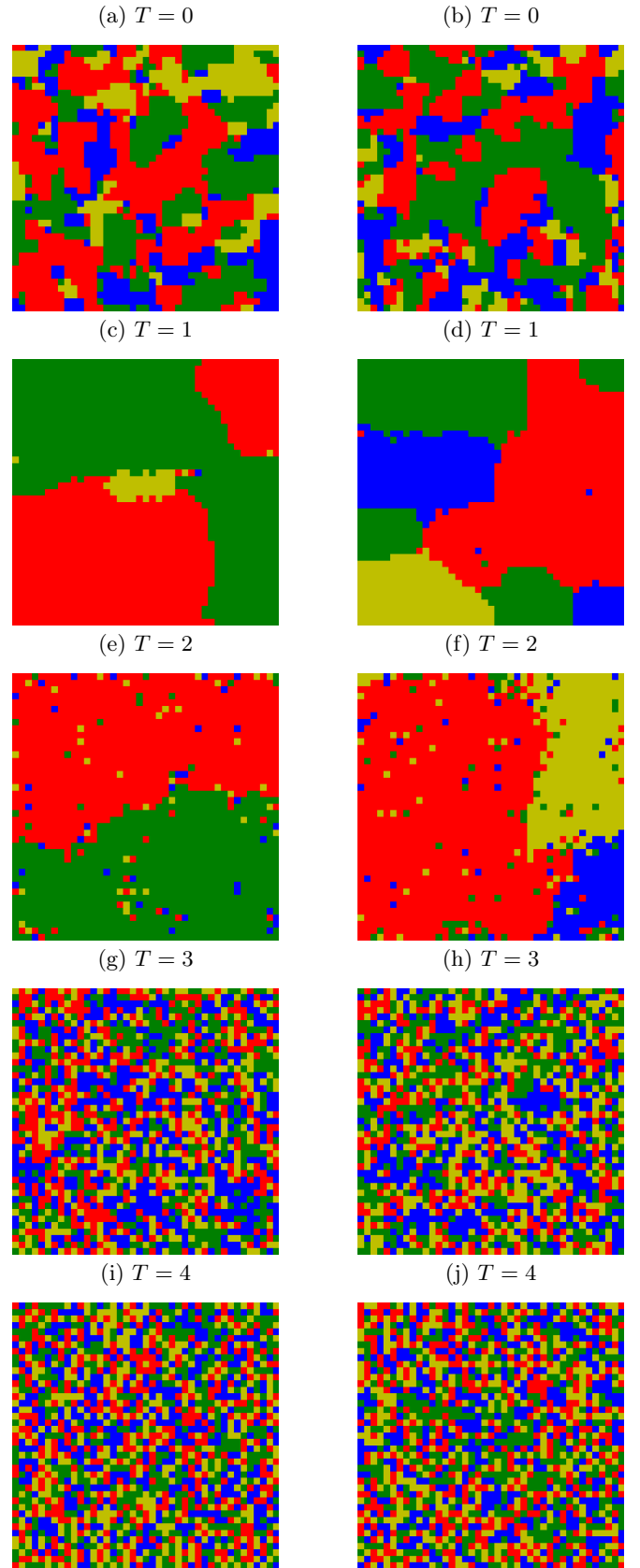


FIG. 13: Examples of two most probable spatial distributions of the final opinion after  $10^3$  time steps.  $L = 41$ ,  $\alpha = 4$ ,  $K = 4$  and various levels of noise  $T$ .



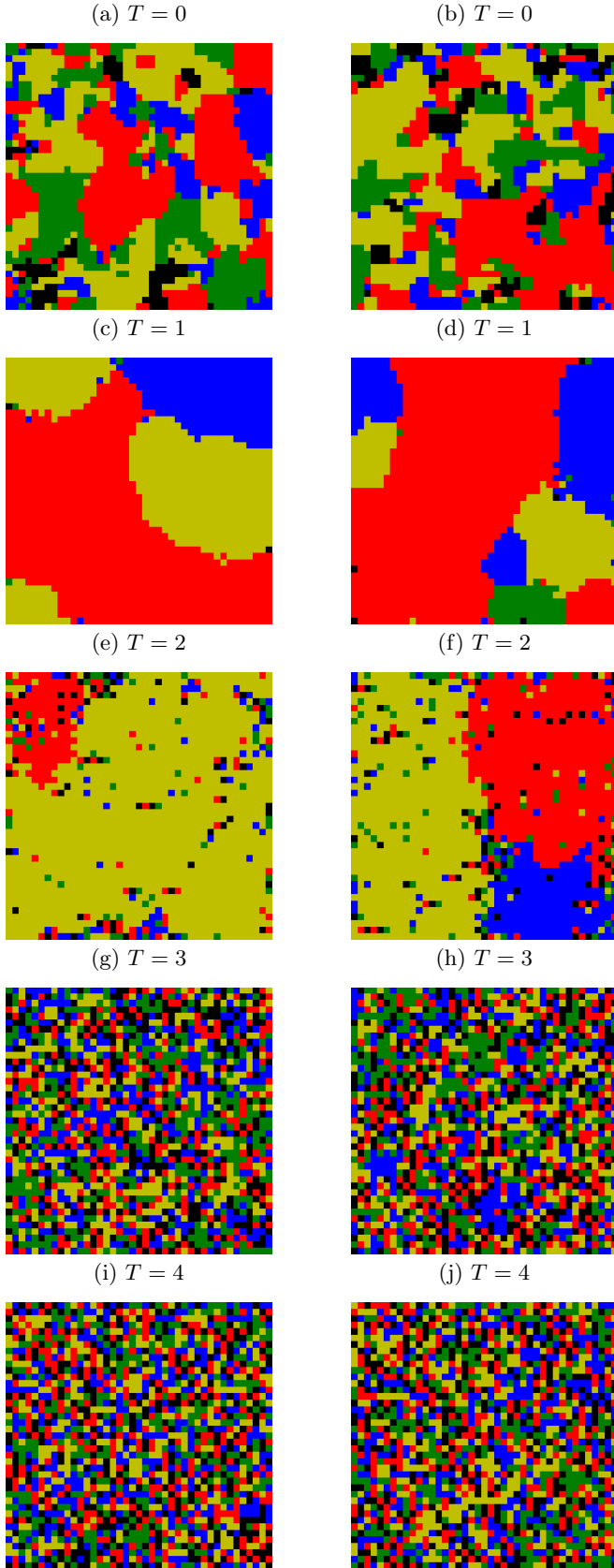


FIG. 14: Examples of two most probable spatial distributions of the final opinion after  $10^3$  time steps.  $L = 41$ ,  $\alpha = 4$ ,  $K = 5$  and various levels of noise  $T$ .

## Appendix B: Average number of clusters

Average number  $\langle C \rangle$  of opinion clusters after  $t = 10^3$  time steps for various exponents of the distance scaling function  $\alpha$  and various numbers  $K$  of opinions available in the system. Noise discrimination threshold  $\theta = 12$  (Figure 15),  $\theta = 25$  (Figure 16),  $\theta = 50$  (Figure 17). The system contains  $L^2 = 41^2$  actors. The results are averaged over  $R = 100$  independent system realisations.

## Appendix C: The number of surviving opinions

Histograms of the frequencies  $f$  of the number  $\Phi$  of surviving opinions after  $= 10^3$  time steps and for various values of the distance scaling function exponent  $\alpha$  and various values of the number of available opinions  $K$ . The system contains  $L^2 = 41^2$  actors. The noise discrimination level  $\theta = 12$  (Figure 18),  $\theta = 25$  (Figure 19),  $\theta = 50$  (Figure 20) and the results are averaged over  $R = 100$  independent simulations.

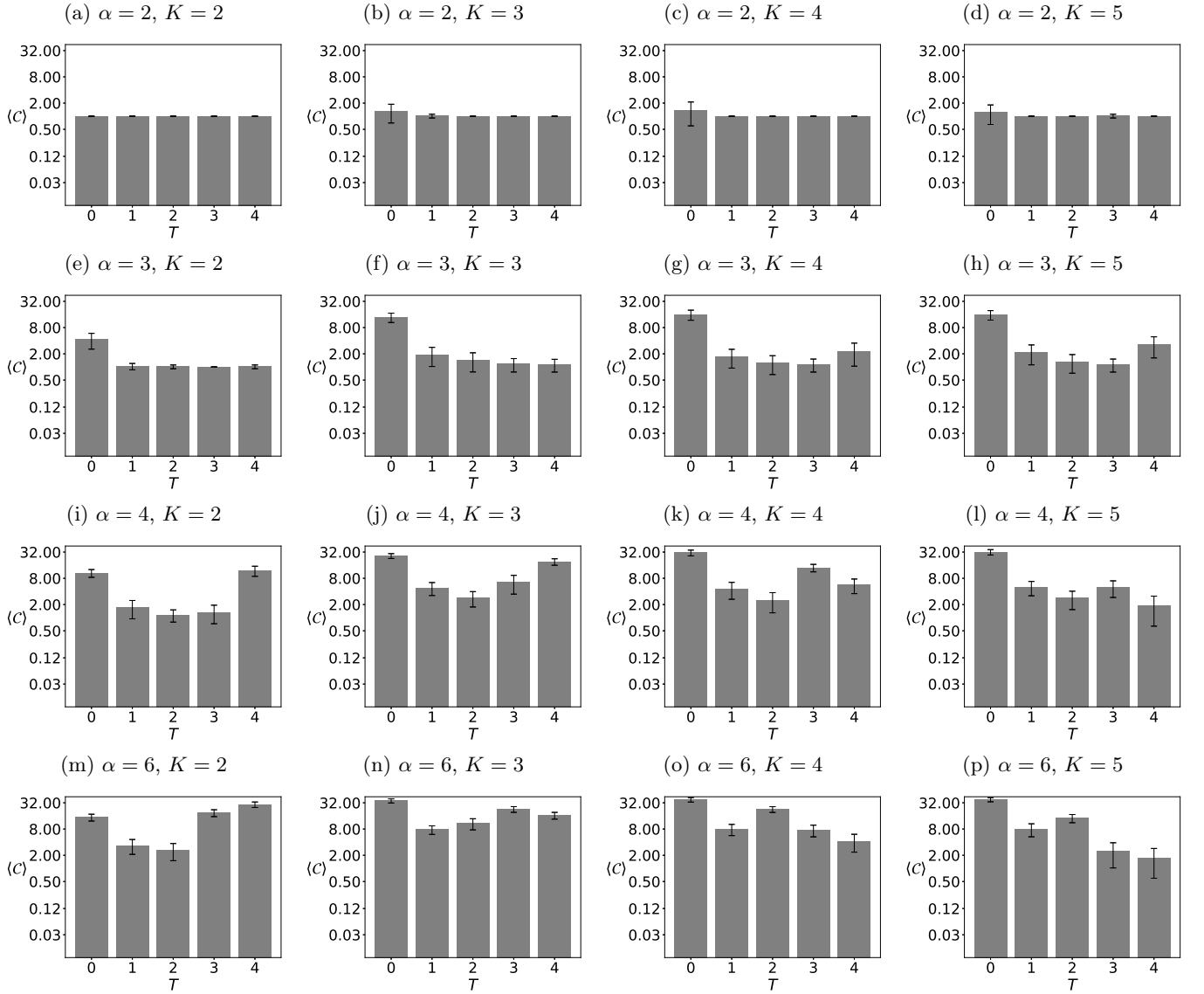


FIG. 15: Average number  $\langle C \rangle$  of opinion clusters after  $t = 10^3$  time steps for various exponents of the distance scaling function  $\alpha$  and various numbers of available opinions  $K$  in the system. Noise discrimination threshold  $\theta = 12$ . The system contains  $L^2 = 41^2$  actors. The results are averaged over  $R = 100$  independent system realizations.

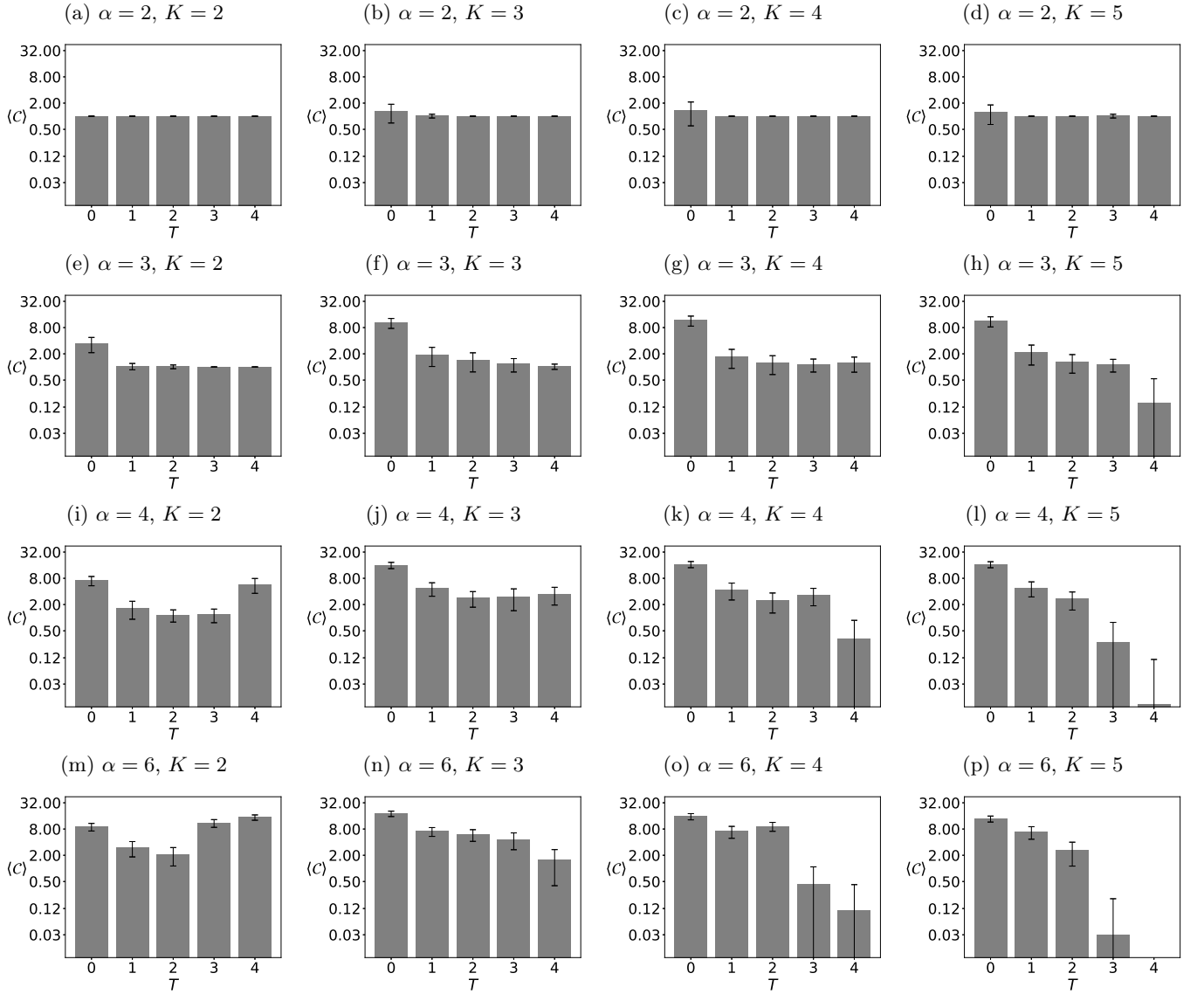


FIG. 16: Average number  $\langle \mathcal{C} \rangle$  of opinion clusters after  $t = 10^3$  time steps for various exponents of the distance scaling function  $\alpha$  and various numbers of available opinions  $K$  in the system. The noise discrimination threshold  $\theta = 25$ . The system contains  $L^2 = 41^2$  actors. The results are averaged over  $R = 100$  independent system realizations.

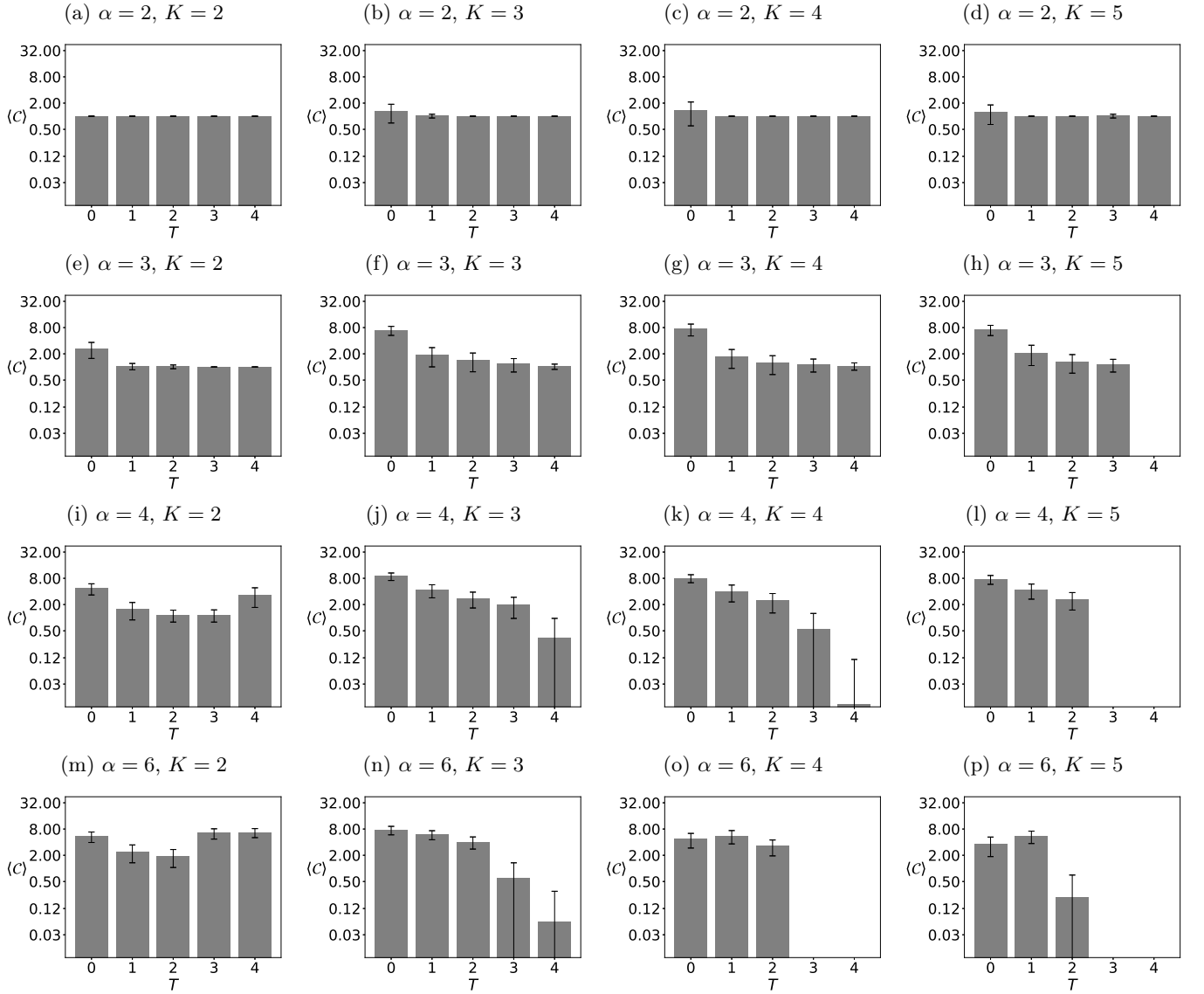


FIG. 17: Average number  $\langle \mathcal{C} \rangle$  of opinion clusters after  $t = 10^3$  time steps for various exponents of the distance scaling function  $\alpha$  and various numbers of available opinions  $K$  in the system. The noise discrimination threshold  $\theta = 50$ . The system contains  $L^2 = 41^2$  actors. The results are averaged over  $R = 100$  independent system realizations.

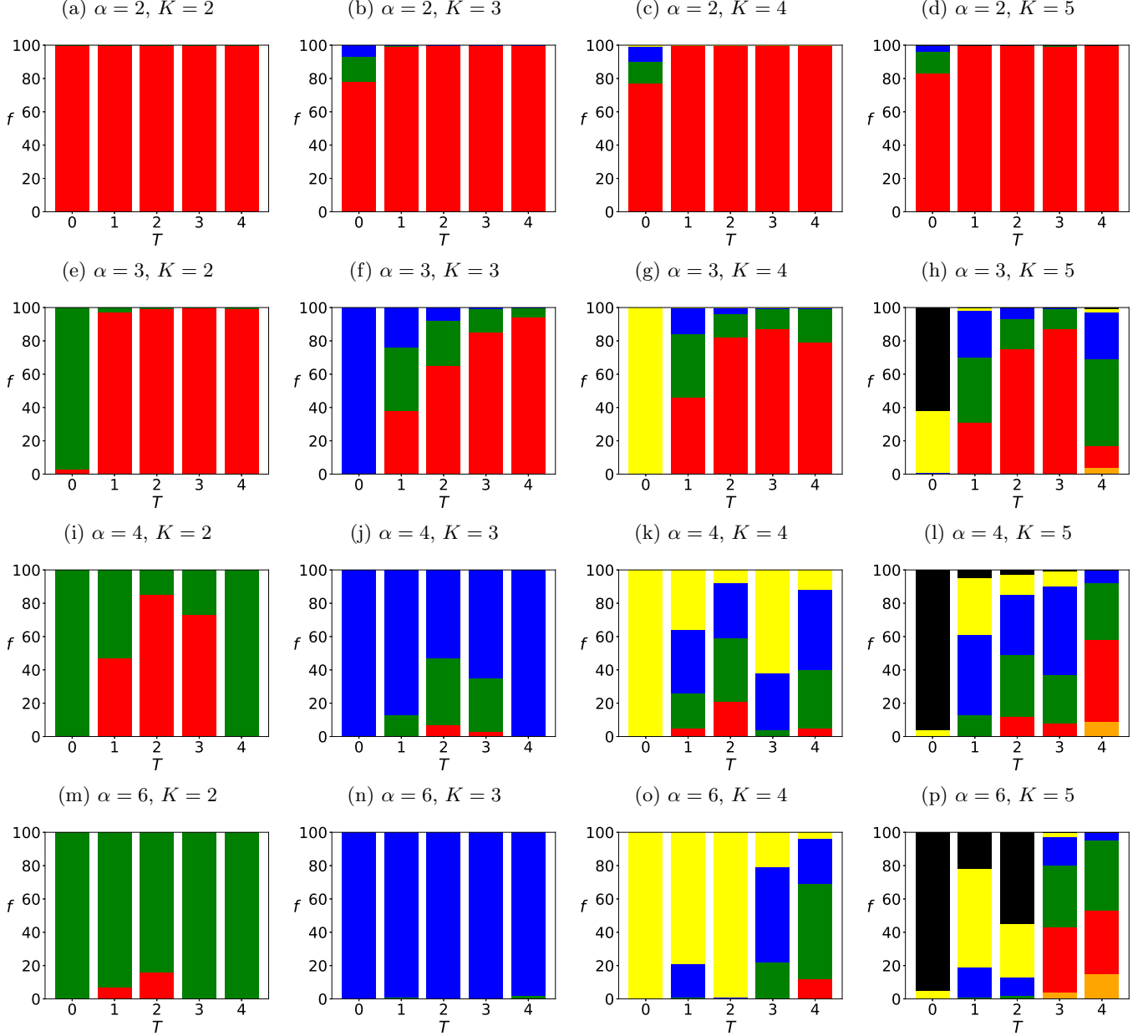


FIG. 18: The histograms of frequencies  $f$  of the number  $\Phi$  of surviving opinions after  $= 10^3$  time steps and for various values of the distance scaling function exponent  $\alpha$  and various values of the number of available opinions  $K$ . The system contains  $L^2 = 41^2$  actors. The noise discrimination level  $\theta = 12$  and the results are averaged over  $R = 100$  independent simulations.

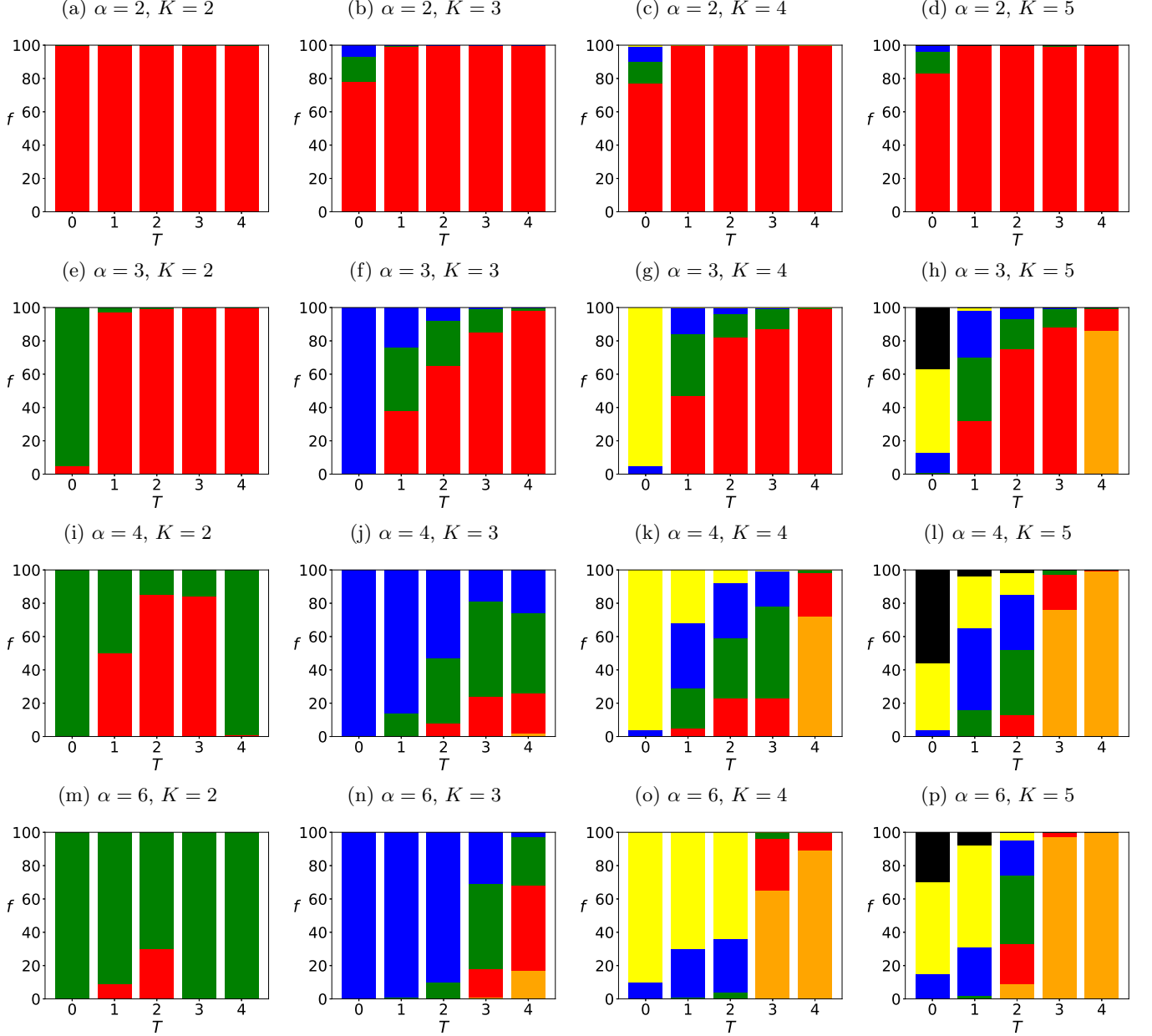
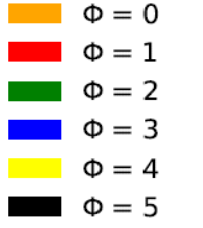


FIG. 19: The histograms of frequencies  $f$  of the number  $\Phi$  of surviving opinions after  $= 10^3$  time steps and for various values of the distance scaling function exponent  $\alpha$  and various values of the number of available opinions  $K$ . The system contains  $L^2 = 41^2$  actors. The noise discrimination level  $\theta = 25$  and the results are averaged over  $R = 100$  independent simulations.

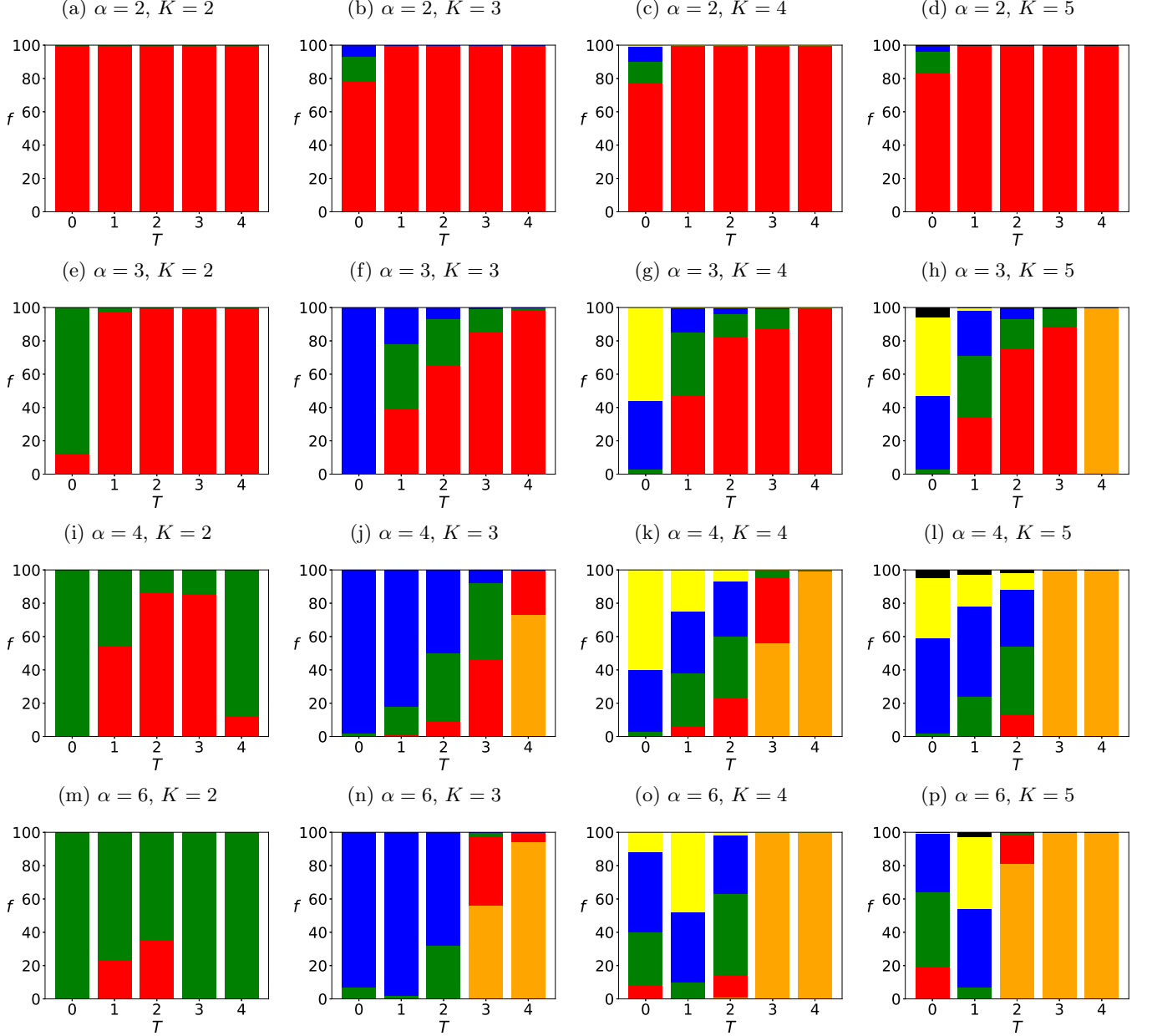
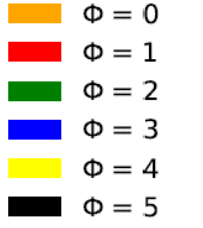


FIG. 20: The histograms of frequencies  $f$  of the number  $\Phi$  of surviving opinions after  $= 10^3$  time steps and for various values of the distance scaling function exponent  $\alpha$  and various values of the number of available opinions  $K$ . The system contains  $L^2 = 41^2$  actors. The noise discrimination level  $\theta = 50$  and the results are averaged over  $R = 100$  independent simulations.